Propagation of Bayesian belief for near-real time statistical assessment of geosynchronous satellite status based on non-resolved photometry data

Anil B Chaudhary, Tamara Payne, Keith Lucas
Applied Optimization, Inc.
Dayton, OH 45402

Kimberly K.J. Kinateder
Wright State University
Dayton, OH 45435

Phan Dao and Jeremy Murray-Krezan
Air Force Research Laboratory, Space Vehicles Directorate
Kirtland AFB, Albuquerque, NM 87117

ABSTRACT

The objective of Bayesian belief propagation in this paper is to perform an interactive status assessment of geosynchronous satellites as each new data point for the photometric brightness becomes available during the synoptic search performed by a space-based sensor as a part of its routine metric mission. The calculations are performed by using a dimensionless ratio of observed photometric brightness to its predicted brightness. The brightness predictions can be obtained using any analytical model chosen by the user. The inference for a level of confidence in the statistical assessment is performed on the basis of propagated values for belief within a cluster of satellites that are located within a close proximity to each other. This is meant to render the assessment to be as independent of assumptions and algorithms utilized in the analytical model as possible; and to mitigate the effect of bias that could be introduced by the choice of analytical model. It considers that a model performs predictions based on the geometry of observation conditions and any information that could have been extracted by the inversion of prior data on its photometric brightness. Thus, if there is a statistical change in the predictive error for a single satellite or a pair of satellites, while remaining unchanged for the rest, there is higher likelihood of anomaly in either the operational status of that satellite or an error in object correlation (i.e. cross-tag).

The algorithm in this paper uses a first order Markov chain model to compute a conditional probability value for the satellite status to be nominal or anomalous (i.e., NOM or ANOM), given its latest photometry observation. This calculation is repeated as data for each new observation becomes available. Also, it is performed for each satellite (member) that belongs to a geosynchronous cluster (group). This provides a sequence of conditional probability values for each member in a group. This information is mapped to a tree-like directed graph (i.e. Bayesian network) of nodes. There is a node for each new data point and it represents a hypothesis test for whether the member status is NOM or ANOM at the time of that observation. The conditional probability values for the status of each member in the group are utilized in order to compute the marginal probability (i.e. belief) that the status of an individual member is NOM or ANOM. The propagation of belief summarizes all preceding computations of belief in order to determine a level of confidence in the statistical assessment for its use by an analyst.

Report Documentation Page		*Form Approved* *OMB No. 0704-0188*

Public reporting burden for the collection of information is estimated to average 1 hour per response, including the time for reviewing instructions, searching existing data sources, gathering and maintaining the data needed, and completing and reviewing the collection of information. Send comments regarding this burden estimate or any other aspect of this collection of information, including suggestions for reducing this burden, to Washington Headquarters Services, Directorate for Information Operations and Reports, 1215 Jefferson Davis Highway, Suite 1204, Arlington VA 22202-4302. Respondents should be aware that notwithstanding any other provision of law, no person shall be subject to a penalty for failing to comply with a collection of information if it does not display a currently valid OMB control number.

1. REPORT DATE **SEP 2014**	2. REPORT TYPE	3. DATES COVERED **00-00-2014 to 00-00-2014**
4. TITLE AND SUBTITLE **Propagation of Bayesian Belief for Near-real Time Statistical Assessment of Geosynchronous Satellite Status Based on Non-resolved Photometry Data**		5a. CONTRACT NUMBER
		5b. GRANT NUMBER
		5c. PROGRAM ELEMENT NUMBER
6. AUTHOR(S)		5d. PROJECT NUMBER
		5e. TASK NUMBER
		5f. WORK UNIT NUMBER
7. PERFORMING ORGANIZATION NAME(S) AND ADDRESS(ES) **Air Force Research Laboratory,Space Vehicles Directorate,Kirtland AFB,NM,87117**		8. PERFORMING ORGANIZATION REPORT NUMBER
9. SPONSORING/MONITORING AGENCY NAME(S) AND ADDRESS(ES)		10. SPONSOR/MONITOR'S ACRONYM(S)
		11. SPONSOR/MONITOR'S REPORT NUMBER(S)
12. DISTRIBUTION/AVAILABILITY STATEMENT **Approved for public release; distribution unlimited**		
13. SUPPLEMENTARY NOTES **In the Advanced Maui Optical and Space Surveillance Technologies (AMOS) Conference, 9-12 Sep 2014, Maui, HI.**		

14. ABSTRACT

The objective of Bayesian belief propagation in this paper is to perform an interactive status assessment of geosynchronous satellites as each new data point for the photometric brightness becomes available during the synoptic search performed by a space-based sensor as a part of its routine metric mission. The calculations are performed by using a dimensionless ratio of observed photometric brightness to its predicted brightness. The brightness predictions can be obtained using any analytical model chosen by the user. The inference for a level of confidence in the statistical assessment is performed on the basis of propagated values for belief within a cluster of satellites that are located within a close proximity to each other. This is meant to render the assessment to be as independent of assumptions and algorithms utilized in the analytical model as possible; and to mitigate the effect of bias that could be introduced by the choice of analytical model. It considers that a model performs predictions based on the geometry of observation conditions and any information that could have been extracted by the inversion of prior data on its photometric brightness. Thus, if there is a statistical change in the predictive error for a single satellite or a pair of satellites, while remaining unchanged for the rest, there is higher likelihood of anomaly in either the operational status of that satellite or an error in object correlation (i.e. cross-tag). The algorithm in this paper uses a first order Markov chain model to compute a conditional probability value for the satellite status to be nominal or anomalous (i.e., NOM or ANOM), given its latest photometry observation. This calculation is repeated as data for each new observation becomes available. Also, it is performed for each satellite (member) that belongs to a geosynchronous cluster (group). This provides a sequence of conditional probability values for each member in a group. This information is mapped to a tree-like directed graph (i.e. Bayesian network) of nodes. There is a node for each new data point and it represents a hypothesis test for whether the member status is NOM or ANOM at the time of that observation. The conditional probability values for the status of each member in the group are utilized in order to compute the marginal probability (i.e. belief) that the status of an individual member is NOM or ANOM. The propagation of belief summarizes all preceding computations of belief in order to determine a level of confidence in the statistical assessment for its use by an analyst.

15. SUBJECT TERMS

16. SECURITY CLASSIFICATION OF:			17. LIMITATION OF ABSTRACT	18. NUMBER OF PAGES	19a. NAME OF RESPONSIBLE PERSON
a. REPORT **unclassified**	b. ABSTRACT **unclassified**	c. THIS PAGE **unclassified**	**Same as Report (SAR)**	**37**	

1. INTRODUCTION

The method reported in this work is constructed as teamwork of three analytical procedures; namely (1) A procedure to perform inversion of non-resolved photometry data for the brightness of three-axis stabilized geosynchronous satellites. This inversion solves for the individual albedo-area products for the satellite body and its solar panels as a function of their respective observation geometry. The observation geometry is defined separately for the body and panel in terms of their respective angles for the direction of illumination and the sensor line of sight. This procedure is denoted as Inversion Model; (2) A procedure to predict the brightness of a geosynchronous satellite at a given future epoch using the computed values for the albedo-area products for the satellite body and its solar panels. This procedure is denoted as Predictive Model; (3) A method to perform statistical assessment in near-real time. This is denoted as Statistics Model and it is the focus of the present paper. The Inversion and Predictive Models are collectively denoted as Photometry Model. The notation used is defined in Appendix A in addition to the first time it appears in the technical description.

The Statistics Model is independent of the Inversion Model and the Predictive Model. Each model is constructed as a reusable entity. The orchestration of teamwork between the three models is performed within the Statistics Model and it is denoted as Control Logic. The flow chart for the Control Logic is shown in Section 16. The Photometry Model is assumed to be imperfect but invariant. It is imperfect in that its accuracy changes from one satellite to another and from one observation geometry to another. It is invariant in that its analytical competence is fixed. This work uses the Photometry Model reported in References 1-3. It is constructed using the principle of material frame indifference, which allows the same mathematics to be useful for the processing of ground-based or space-based sensor data. This model is implemented as an object-oriented software application [Reference 25]. The Statistics Model is newly implemented as its reusable entity within the same software.

The present work is constructed such that its models are useful for the processing of brightness data collected during the routine metrics mission performed by the existing ground or space-based sensors in the space surveillance network. This is a synoptic search operation and it is the workhorse for the maintenance of geosynchronous satellite catalog. The synoptic search data includes both angles-only metric data and single-point visual, panchromatic brightness data. The positional information for the satellites is derived from the angles-only data and is utilized today for satellite catalog maintenance. The optical cross-section and orientation information for the satellites can be derived from the single point panchromatic brightness data, but this information is neither used nor calculated at present even though the metric data is not sufficient by itself to maintain accurate satellite catalog due to the overcrowding of the geosynchronous (GEO) belt [e.g. Reference 12]. There are two reasons why the single point brightness data (or just 'Brightness data' or 'Brightness' for short) is not used as follows:

The first reason is that photometry analyses are traditionally performed using signature data (denoted as 'Signature Data' in this work) collected using dedicated ground-based sensors. Such Signature Data is typically at a rate of one or more observations per minute. It extends for several minutes or even hours, vividly displaying a clear temporal character of satellite signatures to a human eye [Reference 29]. On the contrary, Brightness Data is collected at a rate two orders of magnitude slower, hiding the same knowledge in bits and pieces in the sparseness. Considering that the solar phase angle changes 15° per hour, if each observation was separated by 90-minutes (which is about equal to the orbital period for a notional space-based sensor in LEO), the successive points in the Brightness data may be considered to be separated by about 22.5° in phase angle. In addition, there is no data during daytime (Figure 1.1). A new formulation of mathematics is required to quilt this knowledge together, particularly in the case of space-based data.

The second reason is that the mathematics of inversion of photometry comprises more unknowns than the number of independent equations. Thus, a mathematical proof cannot be offered for uniqueness of solution, except in special situations. This lack of uniqueness translates into lack of confidence in the inference derived from the solution. A new formulation of mathematics is required to gain the requisite level of confidence through a mathematical evolution of belief (i.e. belief propagation or BP) derived from a sequence of inversions of Brightness Data.

The first reason can be addressed by formulating the governing equations for inversion of Brightness Data using the principle of material frame indifference (PMFI) [References 1-3]. This work draws upon the hidden richness of information in the Brightness data as compared to the traditional Signature Data. Signature Data has higher frame rate that spans the full range of longitudinal phase angles, but for a single value of solar declination. Brightness data

has a much slower frame rate, but it samples the full range of longitudinal phase angle, solar declination and, in the case of space-based data, also the full range of latitudinal phase angles. Assuming a new Brightness Data point was collected every 90 minutes, there are ~3000 data points collected during the nightly operations each year that sample the entire accessible range space for the vector directions of solar illumination and sensor observations for a satellite. The record of Brightness Data represents SSA information…hidden in plain sight.

References 1-3 utilize the two-facet model to formulate the governing equations in terms of two satellite-attached reference frames (Section 2). First is attached to the satellite body (Body) and the second to its solar panels (Panels). The Body points to nadir and the Panels track the sun. The vector directions for solar illumination and sensor observations are computed separately for the Body and the Panels. As a result, the Brightness Data is interpreted in terms of entities intrinsic to the bidirectional reflectance distribution functions (BRDF) for the Body and the Panels. Furthermore, the use of the principle of material frame indifference allows a common procedure for the inversion of data collected by ground-base and space-based sensors. The inversion solves for pose-dependent albedo-area values for the satellite, Body and Panels, which can be reused in order to predict the expected value of Brightness for future observations. Or in summary, the two facet model is used in the Inversion Model as well as the Predictive Model. This is fundamental for the statistical assessment as described in the following sections.
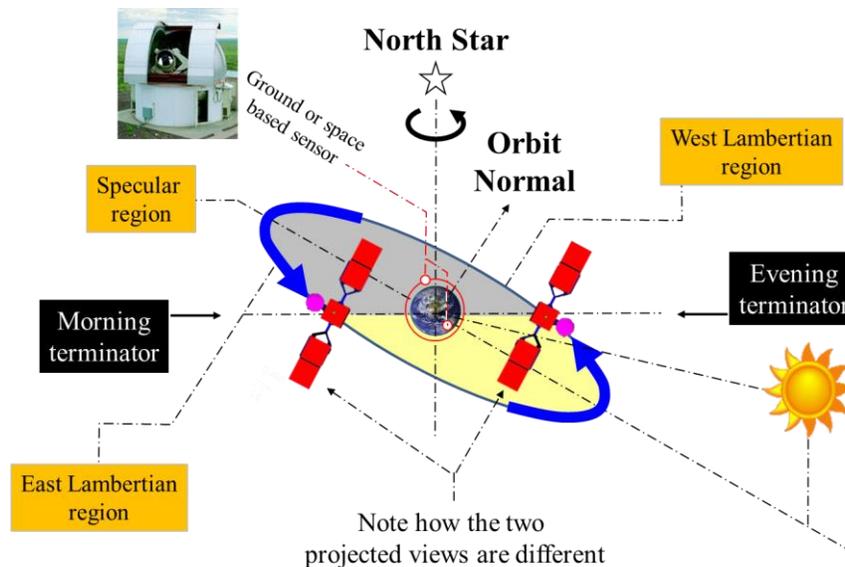
Figure 1.1: An idealized schematic of synoptic search. The West and East designations for the Lambertian regions refer to the direction of illumination.

The second reason can be addressed by using the statistical assessment procedure described in this paper. It draws upon the Bayes network approach described in Reference 4 where each value of a new Brightness Data point is compared with historical values of Brightness Data points under matching conditions of observation geometry in order to assess if the satellite Brightness is nominal (NOM) or anomalous (ANOM). A satellite is NOM from the viewpoint of photometry if its observed Brightness matches with its expected Brightness based on the historical data. A satellite is ANOM otherwise. Such assessment is performed on an ongoing basis in order to visualize continuity in the propagated Bayesian belief, where belief is defined as marginal probability [Reference 5].

The use of historical data for assessment of NOM and ANOM conditions for a satellite presents a peculiar challenge. For example, consider that a satellite Brightness may be denoted as ANOM due to reasons such as cross-tagging with another satellite, visual conjunction, change in the offset angle of its solar panels, 180º turn (yaw rotation) in order to dump momentum, becoming unstable, appearance of unexpected objects in the sensor field-of-view, etc. [References 7-12]. However, for example, cross-tagging arises due to incorrect association and the satellite itself has not become anomalous. Similarly, a change in offset angle or the 180º turn are a part of normal operations and not anomalous behavior. Once the cross-tag is corrected, the new offset-angle is computed, or the 180º turn is recognized, the satellite status would revert back to NOM, although it would be new NOM for which there may or

may not be sufficient historical data available. Also during the period over which the historical data was gathered, , if the satellite was cross-tagged, changed its solar panel offset, etc., the new baseline would become inaccurate.

In order to allow the changing of a satellite status from NOM to ANOM and vice versa, it is essential to possess a consistent baseline which may be used to compute the expected value of Brightness for new observations. Such a baseline can be provided by the Photometry Model. This model can perform inversion of existing Brightness Data and then use the computed albedo-area characteristics to predict the satellite Brightness for new observations that are collected for the directions of illumination and sensor line of sight that may differ from those in the existing data.

Marginal probability or belief is the probability that an outcome for a random variable equals a specific value irrespective of the outcome of the other, correlated random variables [Reference 6]. For example, for jointly distributed random variables X and Y, the marginal probability $P(X = x)$ is given by:

$$P(X = x) = \sum_y P(X = x, \ Y = y) = \sum_y P(X = x \mid Y = y) \ P(Y = y)$$

$$\text{Or,} \quad P(X = x) = \ \mathbb{E}_Y \left[P(X = x \mid Y) \right] \qquad \text{Equation (1)}$$

Where $\mathbb{E}_Y$ denotes the expected value or expectation (i.e. mean) with respect to the probability distribution of Y. Or, the marginal probability for $P(X = x)$ is the expected value for the probability of $X = x$ given that $Y = y$, where all possible values of Y are covered and weighted according to their probabilities and $y_{min} \leq y \ \leq y_{max}$. In the context of denoting the satellite status as NOM or ANOM, it is intrinsic to the satellite itself and is independent of its directions of illumination and the sensor line of sight (i.e., its observation geometry) during the collection of Brightness Data. Thus, the belief that a satellite is NOM or ANOM is the mean probability of NOM or ANOM given any observation geometry. However, there are infinite combinations of observation geometry and the Brightness Data collection is sparse. Thus a compromise is to compute the evolving marginal probability (i.e. belief propagation) for the satellite status in near-real time, as each new point of Brightness Data becomes available.

2. CHARACTER OF BRIGHTNESS DATA

Figure 2a illustrates a notional cluster of geosynchronous satellites (GEO cluster) and how its size compares with a notional field of view (FOV) for a ground or space-based sensor that is utilized for synoptic search. A GEO cluster is defined as a collection of closely-spaced satellites that are station kept within 1° angular subtense of the sky with respect to a ground-based observer [Reference 7]. Thus the size of a typical GEO cluster is smaller than the FOV for a synoptic search sensor and the Brightness Data for the entire GEO cluster can be obtained at the same time.

If a space-based sensor in LEO is to visit each GEO cluster once in each pass, the mean spacing between the Brightness Data points for a GEO cluster will be roughly 90 minutes. In Figure 2.1b, the orbital passes are denoted with symbol k and the temporal spacing between pass (k-1) and k is denoted as Δt_k. The values for the nightly time spacing Δt_k, Δt_{k+1} etc. are expected to be unequal due to differences in sensor tasking between passes. There is a long daytime gap in Brightness Data that spans between the morning and evening terminators. Figure 2.2 illustrates nightly phase angle sampling over three days. For a ground-based sensor, such Brightness Data could be collected with a back-and-forth sweeping motion of the telescope whereby the temporal spacing between successive Brightness Data points varies as a function of the relative position of a GEO satellite with respect to the sensor.

Among the various satellites in a cluster, denoted as C_j, one or more satellites may utilize a bus type different from others and would present themselves with Brightness values that differ significantly from other satellites [Reference 7-8]. In this regard, a difference in excess of 0.3 visual magnitudes or 2% of nominal Brightness may be considered significant [References 10-13]. It is easier to obtain correct tagging for such satellites. References 7-8 discuss potential, human inspection method for differentiating between such satellites with as few as 3 to 5 points of data as long as the three salient regimes of Brightness data are sampled; namely the west Lambertian region, the central specular region, and the east Lambertian region. The west Lambertian region occurs in the hours that follow immediately after the evening terminator. The east Lambertian region occurs in the hours prior to the morning terminator. The Brightness in these regions is dominated by diffuse reflection from the Body and the Panel. The central specular region is closer to midnight and the signature is dominated by specular reflection from the Panel. If a nightly collection was performed once every 90-minutes, approximately eight new data points would be collected per night, with two to three points each in the specular region and in the west and east Lambertian regions.
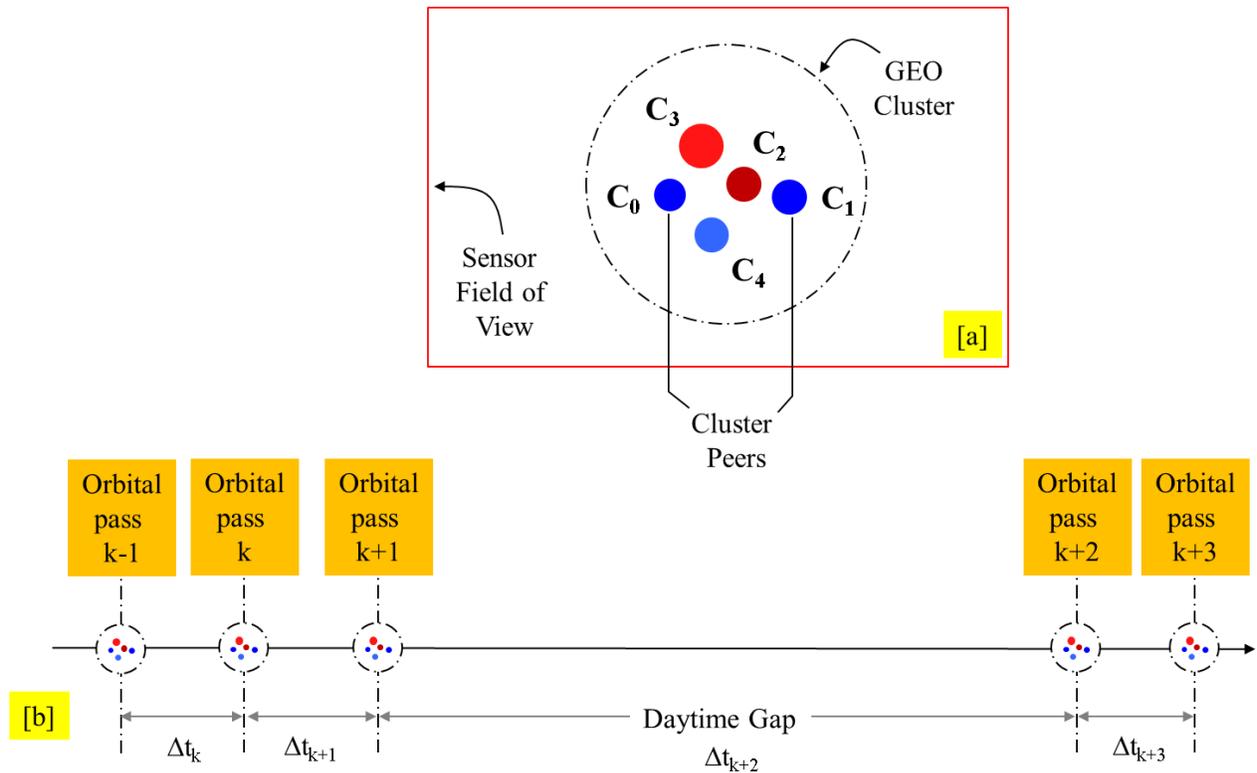
Figure 2.1: [a] Relative size of a notional GEO cluster and sensor field of view (FOV)
[b] Notional collection of one set of Brightness Data per orbital pass or sweep
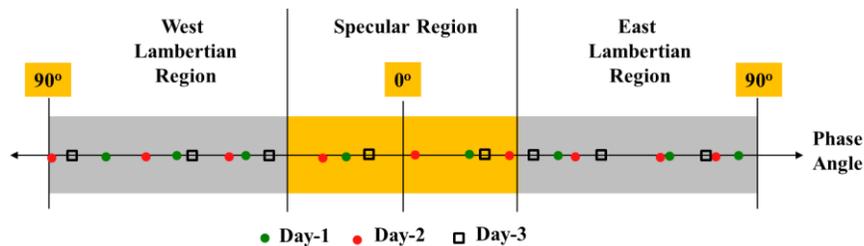
Figure 2.2: Illustration of phase angle sampling over three consecutive days

If the Brightness and/or proximity for satellites C_i and C_j are close, these satellites are denoted as cluster peers [Reference 12]. There is greater potential for cross-tagging between such cluster peers. There can also be a flip-flop in the tagging of cluster peers. In order to mitigate such cross-tagging, the availability of a model for the inversion and prediction of Brightness Data is important in order to support the calculations for statistical assessment.

3. INVERSION AND PREDICTION OF BRIGHTNESS DATA

Due to the variable sensor tasking, orbital motion of the space-based sensor and a continuous change in the solar declination angle, the observation geometry is different for each pass. Also, the satellite operators periodically change the solar panel offset angle and may also subject the spacecraft to 180º turn in order dump momentum. Furthermore, the aging of satellite materials reduces the Brightness of the Body and Panel. As a result, it is necessary to maintain an updated baseline for the nominal Brightness for the satellite. Such a baseline can be extracted by the inversion of Brightness Data using the Photometry Model reported in References 1-3. In this model, the satellite is represented with a two facet model and the data inversion is posed to solve for the intrinsic albedo-areas for the Body and the Panel, as well as the Panel offset angle. The term 'intrinsic' is meant to describe the scaling factors that appear in a BRDF relationship. For example, Lambert's cosine law defines the change of

Brightness as a function of the phase angle. The numerical value of Brightness contribution by the Body and Panel under Lambertian conditions is given by the multiplication of the cosine term with their respective albedo-area values. Once the albedo-area and offset angle are known, it is feasible to predict the satellite Brightness for the observation conditions in the future passes using the analytical expressions of the BRDF for the Body and Panel.

In order to provide a continuously updated baseline, the Photometry Model application is performed using a time slider approach illustrated in Figure 3.1a. The origin of the time slider is positioned at pass $k = 0$, where it is deemed prior knowledge that the satellite is NOM for sufficient number of prior passes. In terms of the notation of Figure 3.1a, the orbital passes that comprise prior data are assigned values of k less than zero. The new data is when k is greater than or equal to zero. The prior data is utilized for the statistical characterization of NOM behavior of the satellite. To this end, it is sufficient if the number of prior passes provide a minimum of thirty points of Brightness Data for each of the three salient regions; namely the west and east Lambertian region and the specular region. At a median rate of two to three points of data per day for the specular and two Lambertian regions, the number of passes in two weeks is expected to provide sufficient data to perform inversion using the two-facet model. The Photometry Model is used for the inversion of the prior data ($k < 0$) and for the prediction of Brightness for the new data ($k \geq 0$).
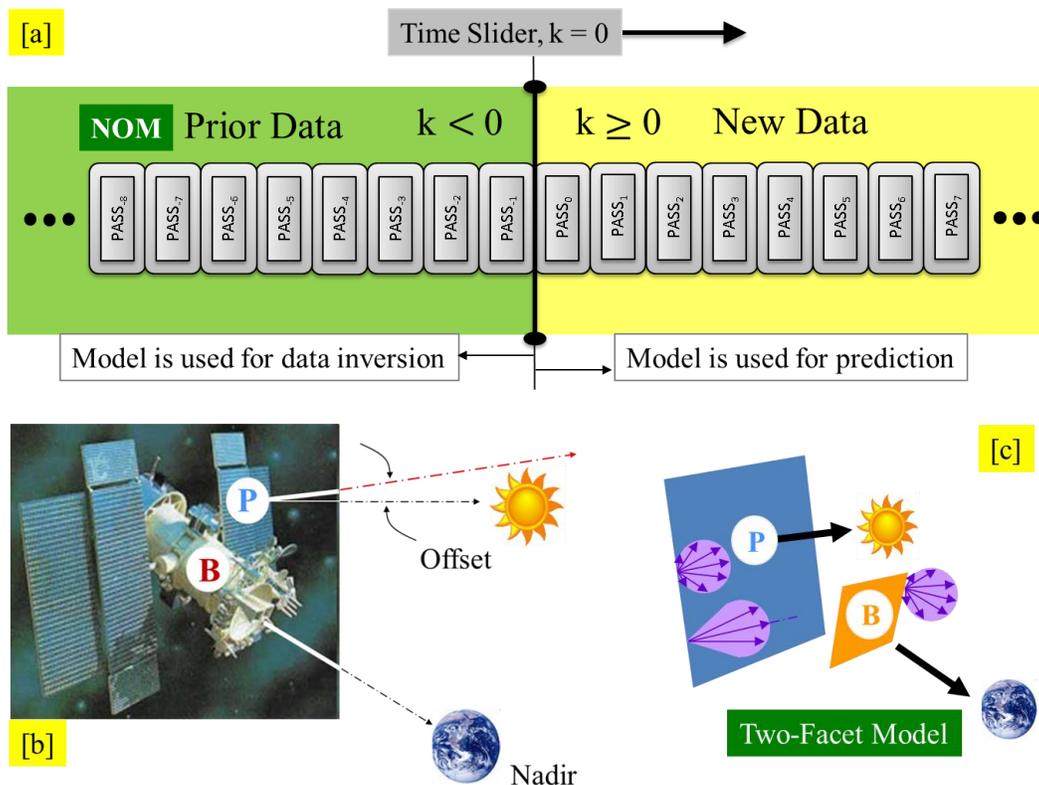
Figure 3.1: [a] Model solution from data inversion on prior data is used to predict brightness for new data
[b] GEO satellite body points to nadir and solar panels track the sun. Offset angle is nonzero
[c] Model extracts Body and Panel albedo areas and offset angle for the Panel from prior data

In order to determine the location of the time slider, it is useful to consider that the statistical assessment is an ongoing process. In order to initialize the assessment, an analyst needs to mark a Brightness Data point as pass $k = 0$ such that the satellite is NOM prior to this pass for a minimum of two weeks. Once the statistical assessment begins, the time slider is moved forward to a temporal position at which the level of belief for NOM status for a satellite fulfills a threshold limit for the level of confidence [Reference 23]. This procedure is described further in Section 15. However, this will result in a different location for the time slider for each satellite in the cluster. Thus, it is simpler to move the time slider only to the largest pass number for which all satellites in the cluster are NOM.

Note that just as the Brightness Data differs from one satellite to another, the Photometry Model accuracy for inversion and prediction also varies from one satellite to another and from one type of observation geometry to another. Indeed, unless proven otherwise, it is useful to assume that the Photometry Model is imperfect and has limited accuracy. Thus, a dimensionless ratio r_{jk} is utilized in order to quantify the difference between the observed and predicted Brightness values. This ratio is denoted as Brightness Ratio. Specifically:

$$r_{jk} = v_{jk} - 1 \qquad \text{Equation (2a)}$$

$$v_{jk} = \frac{I_{ojk}}{I_{mjk}} \qquad \text{Equation (2b)}$$

where I_{ojk} is the Brightness observed for satellite j and pass k, and I_{mjk} is the Brightness predicted by the model for satellite j and pass k. Thus, if the model was a good predictor for satellite j, r_{jk} would be a zero mean random variable. A probability mass function for r_{jk} can now be constructed using prior data (i.e. k < 0). Since r_{jk} is continuous, a continuous, real random variable R is defined such that its range spans all feasible values of r_{jk}.

4. ASSUMPTIONS, INPUT DATA REQUIREMENTS AND OUTPUT

The following assumptions are utilized in this work:

1) The NOM or ANOM state of each satellite is independent of other satellites, except for cluster peers.
2) Cross-tagging is feasible only between cluster peers.
3) The probability that a satellite is NOM or ANOM *during* pass (k+1) depends only on its state *during* pass k and not on its state *during* the passes prior to k. The probability that a satellite is NOM or ANOM *during* pass k depends only on its state *during* pass (k-1) and not on its state *during* the passes prior to (k-1), etc.
4) Each point of observation data for all satellites in a cluster is taken at the same time

Four sets of input data are required as follows:

1) The observations data is available for all satellites in a cluster as soon as it becomes available (i.e., in near real time).
2) The following metadata is provided along with each point observation data: Julian date, Brightness, the coordinates for the satellite, sensor and the sun.
3) The long run probability that a satellite is NOM at any time, π_N. Long run probability means long term probability or probability of NOM irrespective of time, which is the same as marginal probability or belief. This value is estimated by the fraction of passes in the historical data that spans an extended duration (long run historical data) where the state of the satellite is identified as NOM.
4) The terminator-to-terminator transition probability for a satellite. This is probability that the satellite is NOM at the evening terminator given that satellite was NOM at the morning terminator (e.g., this probability is lower for cluster peers that are prone to cross-tag). It is denoted by ${}_N^N T_{Gap}$ where the subscript Gap is in reference to the lack of data during this extended period of time. This is estimated by the fraction of days in the long run historical data when the satellite is denoted as NOM at the last pass for the night at the morning terminator and then denoted as NOM at the first pass for the following evening terminator.

Note that the estimated values for long run probability π_N and terminator-to-terminator transition probability ${}_N^N T_{Gap}$ are based on prior or historical data. They are defined by the user. They can be season or age dependent for each satellite. They can be reset by the user in the midst of a long-term, continuous statistical assessment whereby the updated values are utilized for all points of Brightness Data thereafter.

The output comprises a numerical value for a measure of belief in the NOM or ANOM state of each satellite in a GEO cluster. This output is expected to become available within minutes after the receipt of each new point of Brightness Data. The utility of the ANOM notification is to inform a user that the statistical assessment has detected evidence that the Brightness Ratio is different from when the satellite was NOM. The ANOM notification can also include a likely cause for this difference.

5. PRIOR PROBABILITY DISTRIBUTION FUNCTIONS FOR THE BRIGHTNESS RATIO

The probability distribution function (PDF) for the Brightness Ratio, calculated using the prior data (or, prior PDF) is needed as baseline for the assessment of occurrence of ANOM status in the new data (Figure 3.1). This calculation is at the heart of the statistical assessment. The prior PDF is required for both NOM and ANOM conditions. A procedure for the calculation of the NOM and ANOM PDFs is described in the following:

Since the satellite is deemed NOM prior to the placement of the time slider, the prior PDF for NOM can be calculated using the Brightness Ratio data for passes k < 0. A continuous two week period for the prior data is expected to provide over a hundred values of NOM data for Brightness Ratio. These values will be distributed over the west and east Lambertian and specular regions. A longer period of prior data could be considered, but it is not a requirement. This is because there are limits on how long a continuous stretch of NOM prior data can be feasible on a routine basis. For example, if two cluster peer satellites can become cross-tagged frequently, the mean duration of time when these satellites are NOM is shorter. As a result of limiting to a relatively short prior region, the prior PDF for the NOM state is, in reality, closer to a probability mass function (PMF), which is estimated by constructing a histogram for the values of the Brightness Ratio. Also,

$$f(r_{jk}) = f(r_{jk} \mid NOM_j) P(NOM_j) + f(r_{jk} \mid ANOM_j) P(ANOM_j) \qquad \text{Equation (3)}$$

Where

$f(r_{jk})$ is the PDF for the Brightness Ratio for pass k for satellite C_j

$f(r_{jk} \mid NOM_j)$ is the PDF for the Brightness Ratio for pass k given the satellite C_j is NOM,

$f(r_{jk} \mid ANOM_j)$ is the PDF for the Brightness Ratio for pass k given the satellite C_j is ANOM,

$P(NOM_j)$ is the long run probability that the satellite is NOM, also denoted as π_N, and

$P(ANOM_j)$ is the long run probability that the satellite is ANOM, also denoted as π_A.

$P(ANOM_j) = 1 - \pi_N$

The calculation of PDF for r_{jk} given ANOM is more detailed because ANOM is defined relative to current state of NOM. Also, ANOM is a collective term for a variety of conditions. Assuming that these conditions are mutually disjoint,

$$P(ANOM_j) = P(OffsetChange_j) + P(CrossTag_j) + P(Turn_j) + P(Unstable_j) + P(UCT_j) \dots$$

<div align="right">Equation (4a)</div>

and $P(OffsetChange_j \mid ANOM_j) = \frac{P(OffsetChange_j)}{P(ANOM_j)}$, $P(CrossTag_j \mid ANOM_j) = \frac{P(CrossTag_j)}{P(ANOM_j)}$, etc. Then,

$$
\begin{aligned}
f(r_{jk} \mid ANOM_j) = {} & f(r_{jk} \mid OffsetChange_j) P(OffsetChange_j \mid ANOM_j) \\
& + f(r_{jk} \mid CrossTag_j) P(CrossTag_j \mid ANOM_j) \\
& + f(r_{jk} \mid Turn_j) P(Turn_j \mid ANOM_j) \\
& + f(r_{jk} \mid Unstable_j) P(Unstable_j \mid ANOM_j) \\
& + f(r_{jk} \mid UCT_j) P(UCT_j \mid ANOM_j) \dots
\end{aligned}
$$

<div align="right">Equation (5a)</div>

Or,

$$
\begin{aligned}
f(r_{jk} \cap ANOM_j) = {} & f(r_{jk} \mid OffsetChange_j) P(OffsetChange_j) \\
& + f(r_{jk} \mid CrossTag_j) P(CrossTag_j) + f(r_{jk} \mid Turn_j) P(Turn_j) \\
& + f(r_{jk} \mid Unstable_j) P(Unstable_j) + f(r_{jk} \mid UCT_j) P(UCT_j) \dots
\end{aligned}
$$

<div align="right">Equation (5b)</div>

Where,

$P(OffsetChange_j)$ is the long run probability of change in the panel offset angle for satellite C_j

$P(Crosstag_j)$ is the long run probability of cross-tag for C_j

$P(Turn_j)$ is the long run probability of a 180° turn for C_j

$P(Unstable_j)$ is the long run probability that satellite C_j is unstable

$P(UCT_j)$ is the long run probability of a mistag for C_j due to the appearance of UCT in the sensor FOV

And,

$f(r_{jk} \mid OffsetChange_j)$ is the PDF of Brightness Ratio when the C_j panel offset is modified

$f(r_{jk} \mid CrossTag_j)$ is the PDF of Brightness Ratio when C_j is cross-tagged with a peer

$f(r_{jk} \mid Turn_j)$ is the PDF of Brightness Ratio when C_j is turned 180°

$f(r_{jk} \mid Unstable_j)$ is the PDF of Brightness Ratio when Cj is unstable

$f(r_{jk} \mid UCT_j)$ is the PDF of Brightness Ratio when a mistag is caused by an unexpected UCT

The long run probability values for the anomalous conditions can be identified from the Brightness Ratios for the historical data because each condition has a tell-tale feature. In order to locate these features, it is necessary to consider plots of Brightness Ratio versus phase angle for each night of historical data. These plots can be generated automatically and visualized in order to locate specific anomalies based on their features as described below:

- Change in the solar panel offset causes the Brightness Ratio to become anomalous only in the specular region. The Brightness Ratio in the west and east Lambertian regions is minimally affected because the Panels are highly specular and the effect of offset angle change fades significantly at high phase angles. Thus $P(OffsetChange_j)$ equals the fraction of passes in the historical data where the Brightness Ratio is ANOM only in the specular region.
- Occurrence of cross-tag causes the Brightness Ratios for cluster peers to become anomalous simultaneously. Thus, $P(CrossTag_j)$ equals the fraction of passes in the historical data where the Brightness Ratio has become simultaneously anomalous for the cluster peers. It would also be feasible to verify the cross-tag. For example, let satellite C_i and C_j be the cluster peers that cross-tag. Then the Brightness Ratio for C_i could be recomputed using the term I_{mjk} instead of I_{mik} and vice versa for C_j. This would render the Brightness Ratio NOM if the peers were cross-tagged.
- The effect of 180° yaw turn by a satellite causes the sides of the Body to switch with respect to the illumination by sunlight as illustrated in Figure 5.1. Imagine that the satellite is shown in a pass prior to the 180° yaw turn. The normal to one of the body facets points eastwards. Upon the 180° yaw turn, this normal will point westwards. Thus, the ANOM status resulting from a 180° yaw turn causes the values of Brightness Ratio to switch. The values that normally occurred in the west Lambertian region will now appear in the east Lambertian region, and vice versa (Figure 1.1). Thus $P(Turn_j)$ equals the fraction of passes in the historical data where the Brightness Ratio is ANOM in a manner that depicts an east-west switch.
- Effect of gross instability is loss of attitude control. This creates opportunities for the occurrence of specular glints in the west and east Lambertian regions and the occurrence of diffuse reflection conditions in the specular regions. Thus, the ANOM status for gross instability is plausible if the values of high Brightness are uncorrelated to the phase angle. Thus $P(Unstable_j)$ equals the fraction of passes in the historical data where the Brightness Ratio is ANOM in a manner that depicts lack of correlation with the phase angle.
- A orbital debris in LEO or a higher orbit with its velocity vector aligned with the view direction for a ground or space-based sensor can cause presence of a UCT (i.e. an extra object in close proximity of a GEO cluster), potentially resulting in a mistag when the object association is performed based only on metric data. The same UCT is unlikely to be present the next time the sensor visits the GEO cluster and the error due to incorrect association may or may not be rectified. Indeed, another UCT may appear subsequently and propagate the cycle of incorrect association further [Reference 10]. Thus a situation where the Brightness Ratio is anomalous in one pass but is nominal in the subsequent passes may be due to a UCT that appears momentarily in the sensor field of view. Thus $P(UCT_j)$ equals the fraction of passes in the historical data where the Brightness Ratio is ANOM in a manner that depicts an isolated anomaly.

The calculation procedure for the conditional PDFs (e.g. $f(r_{jk} \mid OffsetChange_j)$) is described in Section 7.
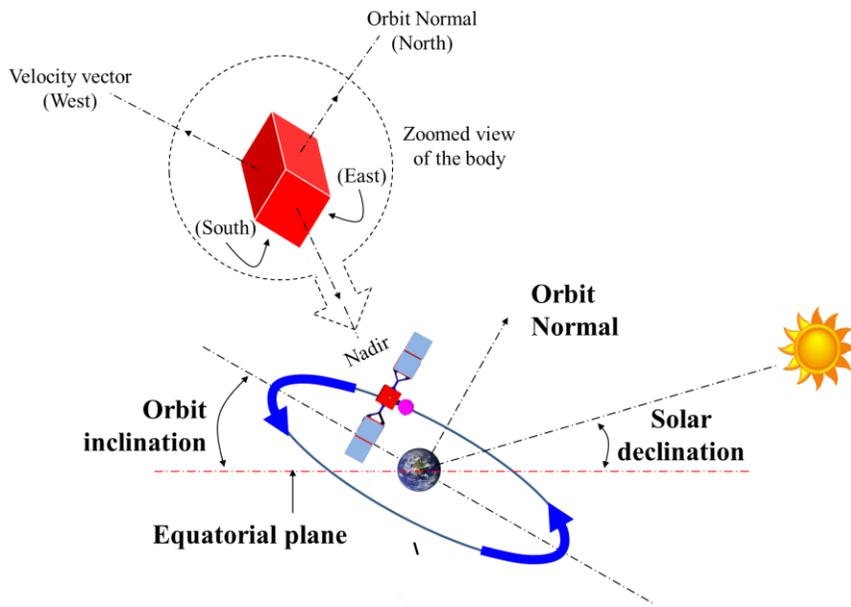
Figure 5.1: Effect of an 180º yaw turn on the orientation of a GEO satellite

6. BAYES NETWORK
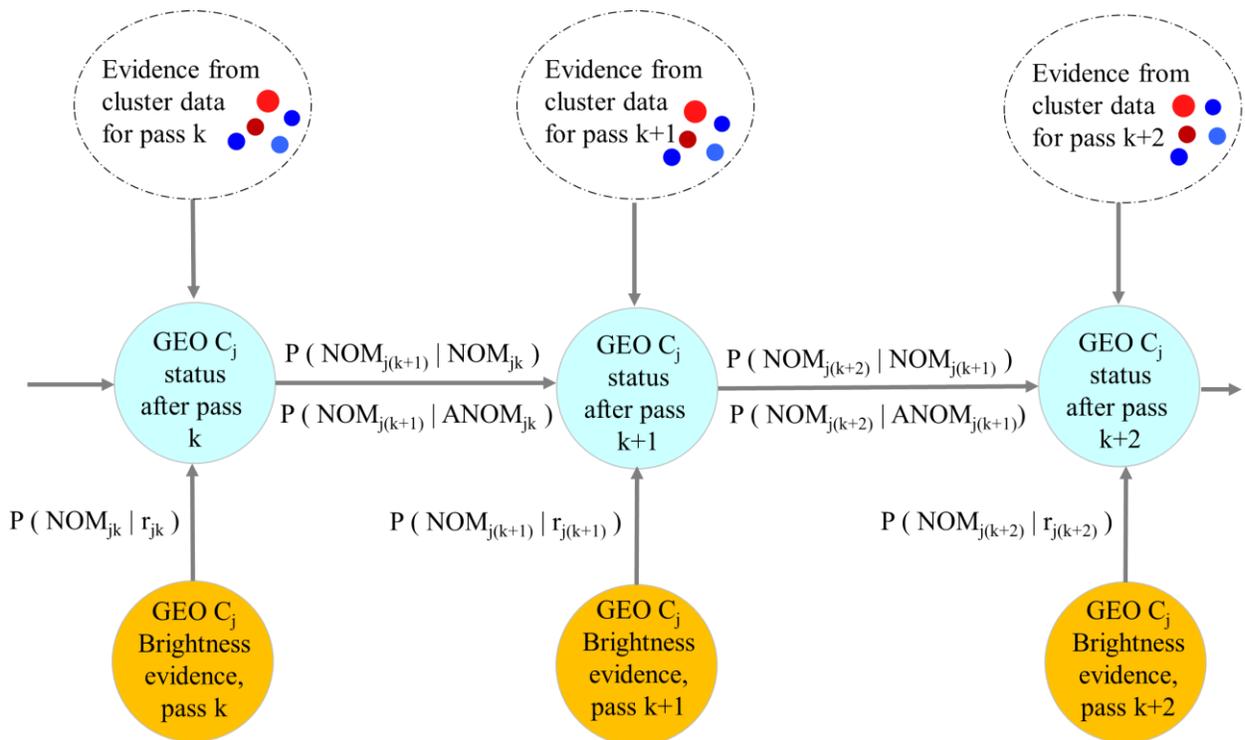
Figure 6.1: Flow of information within the Bayes network for satellite C_j

Figure 6.1 shows a graphical model for the Bayes network to perform statistical assessment of NOM and ANOM status for satellite C_j using Brightness Data. This graphical model builds upon the Bayes network reported in

Reference 4. As in Reference 4, it contains GEO status notes (blue nodes) that receive Brightness evidence (orange nodes) after each pass. The arrows in the network have a direction but they do not loop around. In other words, it is a directed acyclic graph. The network is directional in that it defines the qualitative dependencies between the nodes [Reference 5]. The number of GEO status nodes is equal to the number of passes performed subsequent to the placement of time slider at k = 0. When the time slider is moved forward to a new position, the Bayes Network is reset (Sections 15-16). The GEO status node after pass k is the parent node for the GEO status after pass k+1 and the dependency between nodes is defined in terms of conditional probability. The temporal spacing between the nodes is non-uniform, which corresponds to the time elapsed between the successive collection of Brightness Data points.

In Figure 6.1, $P\left(NOM_{jk} \mid r_{jk}\right)$ is the conditional probability that the status of satellite C_j is NOM at pass k given the Brightness Ratio for the data collected in pass k. The calculation of this conditional probability is performed using Bayes theorem. This calculation is described in Section 7. The quantity $P\left(NOM_{jk} \mid r_{jk}\right)$ occurs often in the following calculations and it is given a simpler notation, X_{jk}. Note that the notation r_{jk} is meant to imply that the value of the continuous random variable R resides in an infinitesimal neighborhood of a given number r_{jk}. This is because R is a continuous random variable and thus the probability that R exactly equals any given number r_{jk} is zero. This consideration is absent in the case of the probability of NOM or ANOM states because they are discrete.

In Figure 6.1, $P\left(NOM_{j(k+1)} \mid NOM_{jk}\right)$ is the conditional probability that the status of satellite C_j is NOM at the time of collection of data in pass (k+1) given satellite C_j status is NOM at the time of collection of data in pass k. The term $P\left(NOM_{j(k+1)} \mid ANOM_{jk}\right)$ is the conditional probability that the status of satellite C_j is NOM at the time of collection of data in pass (k+1) given satellite C_j status is ANOM at the time of collection of data in pass k. These two terms define the probability of transition of the NOM state during the period when no new data is collected. These two terms are the first column of the transition probability matrix, which is computed using the Markov chain. This calculation is described in Section 8. It uses a simpler notation for the conditional probability terms as follows:

$$_{N}^{N}T_{k+1}^{k} = P\left(NOM_{j(k+1)} \mid NOM_{jk}\right) \qquad \text{Equation 6a}$$

$$_{N}^{A}T_{k+1}^{k} = P\left(NOM_{j(k+1)} \mid ANOM_{jk}\right) \qquad \text{Equation 6b}$$

This notation uses two subscripts and two superscripts. The left and right superscripts denote the state and pass number, k. The left and right subscripts denote the state and pass number, k+1. Two additional, related terms are defined in Equation 6 and they appear in relation to the Markov matrix calculations in Section 8.

$$_{A}^{N}T_{k+1}^{k} = 1 - _{N}^{N}T_{k+1}^{k} \qquad \text{Equation 6c}$$

$$_{A}^{A}T_{k+1}^{k} = 1 - _{N}^{A}T_{k+1}^{k} \qquad \text{Equation 6d}$$

The flow of information in the network can be visualized using the GEO status node for pass (k+1). The transition probability terms are utilized to compute the probability that the satellite is NOM prior to the collection of data in pass (k+1) based on the probability that the satellite is NOM for pass k. The evidence of Brightness Ratio for the data collected in pass (k+1) is utilized to compute the probability that the satellite is NOM after the data has been collected in pass (k+1). Then the transition probability terms are utilized to compute the probability that the satellite is NOM prior to the collection of data in pass (k+2); etc. This calculation is performed using the Chapman-Kolmogorov equation and the Markov chain, and it is described in Section 9.

In following the Bayes Network directed graph, the numerical value of probability that satellite C_j is NOM evolves with the collection of each new point of Brightness Data. The value of Brightness in each pass is a function of the observation geometry, namely the directions of illumination and the sensor line of sight. Thus, the conditional probability that satellite C_j is NOM after pass k given the Brightness Ratio r_{jk} can also be interpreted as the conditional probability that satellite C_j is NOM after pass k given the observation geometry for pass k.

The probability density function (PDF) for the Brightness Ratio can be quite different from one satellite to another, even if the satellites are cluster peers. This is due to limitation on accuracy that can be achieved by the Inversion Model. An empirical description of this PDF is computed using the data for passes k < 0 and it is used subsequently

to calculate X_{jk} for passes $k \geq 0$. In the case of a cross-tag between cluster peers, the values of X_{jk} get affected simultaneously for both peer satellites. In order to detect such simultaneous changes, it is beneficial to transform the values of X_{jk} to z-score in order to support the calculation of a measure of belief and for hypothesis testing to assess the probabilities of Type I and Type II errors [References 23 and 26].

In order to assign a numerical value to the belief placed in the status of satellite C_j, we need know the conditional probability irrespective of the observation geometry (see Equation 1), which is the marginal probability that satellite C_j is NOM. In order to compute such marginal probability, we need to sample the entire range space of observation geometry at a sufficient number of locations. This is mostly not feasible because the observation geometry is governed by automated tasking for synoptic search by the sensor. As a result, it is necessary to perform an iterative assessment of belief based on a limited number of data points for each satellite in a cluster. This is performed using the standard z-score, calculation of likelihood rations and hypothesis testing (see Sections 11 to 15).

7. BAYES THEOREM

The purpose of the calculations described in this section is to determine the Brightness evidence, X_{jk} (Figure 6.1). In this regard, the probability that satellite C_j is NOM after pass k and the Brightness Ratio resides in an infinitesimal neighborhood of r_{jk} can be defined using the expression for conditional probability in two ways as follows:

$$P\{ NOM_{jk} \cap (r_{jk} \leq R < r_{jk} + \Delta r_{jk}) \} = P(NOM_{jk} \mid (r_{jk} \leq R < r_{jk} + \Delta r_{jk})) P(r_{jk} \leq R < r_{jk} + \Delta r_{jk})$$

Equation 7a

$$P\{ NOM_{jk} \cap (r_{jk} \leq R < r_{jk} + \Delta r_{jk}) \} = P\{ (r_{jk} \leq R < r_{jk} + \Delta r_{jk}) \mid NOM_{jk}\} P(NOM_{jk})$$

Equation 7b

Substituting Equation 7a into Equation 7b and rearranging,

$$P(NOM_{jk} \mid (r_{jk} \leq R < r_{jk} + \Delta r_{jk})) = \frac{P((r_{jk} \leq R < r_{jk} + \Delta r_{jk}) \mid NOM_{jk}) P(NOM_{jk})}{P(r_{jk} \leq R < r_{jk} + \Delta r_{jk})}$$

Equation 8

Equation 8 is now re-written using the probability density function (PDF) for the Brightness Ratio $f(r_{jk})$, which is suitably interpreted as the probability of R taking values in the small neighborhood about the given value:

$$P(NOM_{jk} \mid r_{jk}) = \frac{f(r_{jk} \mid NOM_{jk}) P(NOM_{jk})}{f(r_{jk})}$$

Equation 9a

$$f(r_{jk}) = f(r_{jk} \mid NOM_{jk}) P(NOM_{jk}) + f(r_{jk} \mid ANOM_{jk}) P(ANOM_{jk})$$ Equation 9b

The above derivation is essentially Bayes theorem. The left hand side of Equation 9a is X_{jk}. Equation 9b expresses the denominator of Equation 9a using the law of total probability. The calculation of $P(NOM_{jk})$ is connected to the calculation of transition probability and it is described in Sections 8 and 9.

The conditional PDF $f(r_{jk} \mid NOM_{jk})$ is computed as empirical PDF from the prior data, which is denoted by passes $k < 0$ (Figure 3.1). Note that this is permissible because the time slider is positioned such that the satellite status is NOM for a minimum of two weeks prior to the location $k = 0$. This data is utilized as input to the Inversion Model and for the calculation of r_{jk}. Note that such inversion calculation is performed upon the translation of the time slider to each new position so that the empirical PDF $f(r_{jk} \mid NOM_{jk})$ may evolve with the passage of time.

The $f(r_{jk})$ calculation includes contributions from NOM and ANOM conditions (Equation 3). Note that the first term in Equation 3 is the NOM term, which is the same as the numerator of Equation 9 for pass $k = 0$. The second term in Equation 3 is the ANOM term. It is given by Equation 5a by considering the contributions from five disjoint

anomalies. Among these anomalous states, the CrossTag, Turn, and Unstable are Boolean states. They are either true or false. The OffsetChange and UCT are continuous states. The changed solar panel offset may be any real number within a range of permissible values. The Brightness of a UCT may be any real number, although it will typically be a fainter object. The PDF calculation for the discrete and continuous ANOM states is described in the following based on a combination of arguments derived from the observations data and physical considerations.

The calculation of $f(r_{jk} \mid CrossTag_j)$ is performed as follows. Consider that satellite C_j is incorrectly tagged as its cluster peer, denoted as C_j^{Peer}. Then the Brightness Ratio given CrossTag can be expressed as:

$$v_{jk}^{CrossTag} = \{ I_{mjk} / I_{mjk}^{Peer} \} v_{jk} \qquad \text{Equation 10a}$$

$$r_{jk}^{CrossTag} = v_{jk}^{CrossTag} - 1 \qquad \text{Equation 10b}$$

In Equation 10a, the value of v_{jk} given by Equation 2b. It is scaled by the ratio of predicted Brightness for satellite C_j to the predicted Brightness for satellite C_j^{peer}. The predicted brightness for C_j and C_j^{peer} assume both satellites to be NOM. The resulting values of $r_{jk}^{CrossTag}$ are used to compute the empirical PDF for $f(r_{jk} \mid CrossTag_j)$.

The calculation of $f(r_{jk} \mid Turn_j)$ is performed as follows. Consider that satellite C_j has undergone a 180º yaw turn. The turned satellite is denoted as C_j^{Turn}. Then the Brightness Ratio given Turn can be expressed as:

$$v_{jk}^{Turn} = \{ I_{mjk} / I_{mjk}^{Turn} \} v_{jk} \qquad \text{Equation 11a}$$

$$r_{jk}^{Turn} = v_{jk}^{Turn} - 1 \qquad \text{Equation 11b}$$

In Equation 11a, the value of v_{jk} given by Equation 2b. It is scaled by the ratio of predicted Brightness for satellite C_j to the predicted Brightness for satellite C_j^{Turn}. The rotation of the satellite modifies the Brightness contributions of the Body and Panel to the total Brightness for a satellite as described using Figure 5.1. The modified contributions of the Body and Panel can be computed using the Predictive Model. The modified projected view upon the yaw turn is utilized in order to compute the predicted brightness I_{mjk}^{Turn}. The resulting values of r_{jk}^{Turn} are used to compute the empirical PDF for $f(r_{jk} \mid Turn_j)$.

The calculation of $f(r_{jk} \mid Unstable_j)$ is performed as follows. Consider that satellite C_j becomes unstable and it is now denoted as $C_j^{Unstable}$. Then the Brightness Ratio for the $Unstable$ condition can be expressed as:

$$v_{jk}^{Unstable} = \{ I_{mjk} / I_{mjk}^{Unstable} \} v_{jk} \qquad \text{Equation 12a}$$

$$r_{jk}^{Unstable} = v_{jk}^{Unstable} - 1 \qquad \text{Equation 12b}$$

In Equation 12a, the value of v_{jk} given by Equation 2b. Note that when a satellite is unstable, its projected view with respect to the sensor is independent of the solar phase angle. Or, its Brightness at high phase angles can be larger than that at low phase angles. Thus, in the calculation of $v_{jk}^{Unstable}$, the value of $I_{mjk}^{Unstable}$ is randomly distributed between the maximum and minimum values possible for the Brightness of satellite C_j while in its NOM state. These values are denoted as bounds, which are computed using the Predictive Model. The range for the resulting values for $r_{jk}^{Unstable}$ is a function of the phase angle because I_{mjk} is a single number. These values for $r_{jk}^{Unstable}$ are used to compute the empirical PDF for $f(r_{jk} \mid Unstable_j)$. Note that this PDF also becomes a function of the phase angle.

The calculation of $f(r_{jk} \mid OffsetChange_j)$ is performed as follows. Consider that satellite C_j changes its solar panel offset and it is now denoted as $C_j^{OffsetChange}$. Then the Brightness Ratio for the $OffsetChange$ condition can be expressed as:

$$v_{jk}^{OffsetChange} = \{\; I_{mjk} \,/\, I_{mjk}^{OffsetChange} \,\} \, v_{jk} \qquad \text{Equation 13a}$$

$$r_{jk}^{OffsetChange} = v_{jk}^{OffsetChange} - 1 \qquad \text{Equation 13b}$$

Note that when a satellite changes its Panel offset, the projected view of the Panel with respect to the sensor changes while the projected view of the body remains unchanged. Since the Panels are highly specular, their contribution to the satellite Brightness in both Lambertian regions is small as compared to the Body (Figure 1.1). Or, the value of $v_{jk}^{OffsetChange}$ remains largely unchanged in the Lambertian regions in spite of the change in the offset angle.

In the specular region, $I_{mjk}^{OffsetChange}$ is randomly distributed between the maximum and minimum values of Brightness that can occur for a NOM satellite Cj in the specular region. These maximum and minimum values are computed using the Predictive Model. The range for the resulting values for $r_{jk}^{OffsetChange}$ is then a function of the phase angle in the specular region only. These values for $r_{jk}^{OffsetChange}$ are used to compute the empirical PDF for $f(\, r_{jk} \,|\, OffsetChange_j)$. Note that this PDF is a function of the phase angle during pass k when it is in the specular region. The PDF for $f(\, r_{jk} \,|\, OffsetChange_j)$ for the Lambertian regions is same as that for the NOM state.

The calculation of $f(\, r_{jk} \,|\, UCT_j)$ is performed as follows. This calculation is similar to the *Unstable* state of ANOM. Consider that a UCT is incorrectly tagged as satellite C_j. The incorrectly tagged UCT is now denoted as C_j^{UCT}. Then the Brightness Ratio for the UCT condition can expressed as:

$$v_{jk}^{UCT} = \{\; I_{mjk} \,/\, I_{mjk}^{UCT} \,\} \, v_{jk} \qquad \text{Equation 14a}$$

$$r_{jk}^{UCT} = v_{jk}^{UCT} - 1 \qquad \text{Equation 14b}$$

Typically a UCT would be a faint object that appears unexpectedly in the sensor field of view. The range of Brightness values for such a UCT is a function of the detection limit for the sensor. This range is typically a known value and I_{mjk}^{UCT} is randomly distributed between the range of Brightness for the UCT objects. The range for the resulting values for r_{jk}^{UCT} changes as function of the phase angle. These values for r_{jk}^{UCT} are used to compute the empirical PDF for $f(\, r_{jk} \,|\, UCT_j)$. Note that this PDF also becomes a function of the phase angle.

With the above calculations, all terms on the right hand side of the Bayes expression (Equation 8) are estimable and considered known. This allows the calculation of Brightness evidence, denoted as X_{jk}, which is sent to the GEO status node. Even though this calculation requires the determination of a number of individual terms, it is a minor computational effort for a desktop computer. It is represented by vertical arrows in Figure 6.1. The calculation corresponding to the horizontal arrows is described in Section 8. In this regard, note that

$$P(\, ANOM_{jk} \,|\, r_{jk}) = 1 - P(\, NOM_{jk} \,|\, r_{jk}) \quad \text{Equation 15}$$
$$= 1 - X_{jk}$$

8. TRANSITION PROBABILITY

The purpose of the calculations described in this section is to compute the terms $_N^N T_{k+1}^k$ and $_N^A T_{k+1}^k$, which are shown alongside the horizontal arrows in the Bayes network graph (Figure 6.1). They describe the probability of transition from NOM to NOM or from ANOM to NOM in the interval of time between pass k and pass k+1 when there is no data collected. This interval is denoted as the Inter-pass Time or Δt_k in the following description. Accounting for the probability of change of state during the Inter-pass Time is necessary for the following reasons: (1) The Inter-pass Time, Δt_k can change from one pass to the next by over a magnitude. For example, in case of a ground-based sensor that executes an east-west, back-and-forth sweeping motion to perform synoptic search, the Brightness Data for the satellites located at high zenith angles has an alternating set of large and small values for Δt_k; (2) There is, in effect, no collection of Brightness Data 50% of the time due to the daytime gap; (3) The Δt_k is routinely significant in

comparison to the time required for a satellite to maneuver, to change its solar panel offset, or to execute a 180º yaw turn or (i.e. to transition towards the occurrence of an ANOM state such as CrossTag, OffsetChange or Turn). The Δt_k can also be significant with respect to a duration over which a satellite may experience degradation of its attitude control, progressing towards the occurrence of the ANOM state, Unstable; (4) The Δt_k is significant in order to allow different UCT objects to appear in the successive passes, particularly when the sensor line-of-sight can cross a debris field at an altitude lower than the geosynchronous belt.

For the purpose of this section, assume that Δt_k is constant between all night-time passes and the daytime gap is twelve hours. These assumptions are unnecessary in the actual implementation of the algorithm, but they are useful to simplify the following description. Let the daytime gap be denoted as Δt_{Gap}.

The transition probability matrix $\mathbb{T}$ is defined using the following matrix equation [References 15-17].

$$\mathbb{T} = \begin{bmatrix} {}^N_N T & {}^N_A T \\ {}^A_N T & {}^A_A T \end{bmatrix} \qquad \text{Equation 16}$$

Where

${}^N_N T$ is the probability of persistence of NOM state (i.e. no change) over a unit interval of time
${}^A_N T$ is the probability of transition of ANOM to NOM over a unit interval of time
${}^N_A T$ is the probability of transition of NOM to ANOM over a unit interval of time
${}^A_A T$ is the probability of persistence of ANOM over a unit interval of time

The matrix $\mathbb{T}$ is also called the Markov transition matrix. If $\Delta t_k = 1$, then

$$\begin{bmatrix} {}^N_N T^k_{k+1} & {}^N_A T^k_{k+1} \\ {}^A_N T^k_{k+1} & {}^A_A T^k_{k+1} \end{bmatrix} = \mathbb{T} \qquad \text{Equation 17a}$$

If $\Delta t_k \neq 1$, the Markov transition matrix is computed using the Chapman-Kolmogorov equation [Reference 17]:

$$\begin{bmatrix} {}^N_N T^k_{k+1} & {}^N_A T^k_{k+1} \\ {}^A_N T^k_{k+1} & {}^A_A T^k_{k+1} \end{bmatrix} = \mathbb{T}^{\Delta t_k} \qquad \text{Equation 17b}$$

The $(\Delta t_k)^{th}$ power of the Markov matrix $\mathbb{T}$ is computed using the Cayley-Hamilton theorem [References 18-20]. This comprises a three step procedure: (1) Compute eigenvectors and eigenvalues of $\mathbb{T}$; (2) Raise the eigenvalues to the $(\Delta t_k)^{th}$ power; (3) Compute $\mathbb{T}^{\Delta t_k}$ using the eigenvectors for matrix $\mathbb{T}$ and its eigenvalues raised to the $(\Delta t_k)^{th}$ power. Note that each row of the Markov matrix $\mathbb{T}$ sums to one (see Equations 6c and 6d).

A salient property of a Markov matrix is that its first eigenvalue is equal to 1 [References 18 and 21]. Also the sum of two eigenvalues of $\mathbb{T}$ is equal to the sum of its diagonal elements (i.e. its trace) and the product of the two eigenvalues is equal to the determinant of $\mathbb{T}$. This is because the trace and the determinant of a matrix are its first and third invariant, respectively [Reference 22]. Thus, the two eigenvalues for matrix $\mathbb{T}$, namely λ_1 and λ_2 are given directly by Equation 18 and two eigenvectors are computed by solving two sets of 2x2 simultaneous equations:

$$\lambda_1 = 1 \qquad \text{Equation 18a}$$

$$\lambda_2 = {}^N_N T + {}^A_A T - \lambda_1 \qquad \text{Equation 18b}$$

Using the same logic to the transition probability for the daytime gap by replacing the $(\Delta t_k)^{th}$ power of the Markov matrix $\mathbb{T}$ to the $(\Delta t_{Gap})^{th}$ power:

$$\begin{bmatrix} {}^N_N T_{Gap} & {}^N_A T_{Gap} \\ {}^A_N T_{Gap} & {}^A_A T_{Gap} \end{bmatrix} = \mathbb{T}^{\Delta t_{Gap}} \qquad \text{Equation 19}$$

The matrix elements on the left hand side of Equation 19 are defined in analogous manner as Equation 17b; except that the right superscript and subscript is replaced by the descriptor Gap instead of the pass numbers k and k+1. Note

that $_N^N T_{Gap}$ is user input, as defined in Section 4. This allows the calculation of $_A^N T_{Gap}$ using Equation 6c. However, the matrix elements in the second row of Equation 19 are unknown. They are solved using the user input defined in Section 4 for the long run probability that the satellite is NOM at any time. This is described next.

In the limit, long term is defined as being at least two orders of magnitude longer than Δt_{Gap}, which is 3 to 6 months. The long run probabilities may now be visualized as saturated or steady-state values resulting from successive multiplication of daytime gap transition probability matrix ad infinitum:

$$\begin{bmatrix} \pi_N & (1 - \pi_N) \\ (1 - \pi_A) & \pi_A \end{bmatrix} = \begin{bmatrix} _N^N T_{Gap} & _A^N T_{Gap} \\ _N^A T_{Gap} & _A^A T_{Gap} \end{bmatrix}^{\infty} \qquad \text{Equation 20}$$

Note that π_N is the user input value of long run probability. Note that the rows of both matrices are consistent with Equation 6. However, in the steady state, π_A is also equal to $(1 - \pi_N)$ and thus Equation 20 is singular. It is however, equivalent to a left eigenvector form as follows:

$$\begin{bmatrix} \pi_N & \pi_A \end{bmatrix} = \begin{bmatrix} \pi_N & \pi_A \end{bmatrix} \begin{bmatrix} _N^N T_{Gap} & _A^N T_{Gap} \\ _N^A T_{Gap} & _A^A T_{Gap} \end{bmatrix} \qquad \text{Equation 21}$$

Equation 21 is solved using the user-input values for π_N and $_N^N T_{Gap}$ to determine every term in the equation. Thus, this equation is the starting point for the calculation of the transition probability matrix $\mathbb{T}$ as the $(1/\Delta t_{Gap})^{th}$ root of the transition probability matrix for the daytime gap. This is performed using the Cayley-Hamilton theorem.

Note how the procedure is generalized when Δt_k and Δt_{Gap} are non-uniform. Even though this calculation requires the determination of a number of individual terms, it is a minor computational effort for a desktop computer because it involves a set closed-form analytical procedure; namely the use of Chapman-Kolmogorov equation to calculate the multi-step transition matrices and the use of Cayley-Hamilton theorem to perform this calculation quickly.

9. MARKOV CHAIN

Markov chain is utilized to proceed from one GEO status node to the next by combining the calculations from the application of Bayes theorem and the transition probability. The two calculations taken together allow computation of the term $P(NOM_{j(k+1)})$ using the assumption that the NOM or ANOM state for a satellite during pass k+1 depends only on its state during pass k (Section 4). This is Markov chain of memory 1, or order 1, or simply a first order Markov chain [References 15 and 17]. It is possible to utilize a higher order Markov chain, but it needs joint probability distribution functions. This requires larger amounts of data as input, which conflicts with the user need to produce credible statistical assessment while minimizing the input data required. The first order Markov chain provides matrix equations for the calculation of $P(NOM_{j(k+1)})$ and for the calculation of the numerator in Equation 9 for pass (k+1) as follows:

$$[P(NOM_{j(k+1)}) \quad P(ANOM_{j(k+1)})] = [X_{jk} \quad (1 - X_{jk})] \begin{bmatrix} _N^N T_{k+1}^k & _A^N T_{k+1}^k \\ _N^A T_{k+1}^k & _A^A T_{k+1}^k \end{bmatrix} \qquad \text{Equation 22a}$$

$$f(r_{j(k+1)} \mid NOM_{j(k+1)}) P(NOM_{j(k+1)}) =$$

$$f(r_{j(k+1)} \mid NOM_{j(k+1)})(X_{jk} \, _N^N T_{k+1}^k + (1 - X_{jk}) \, _N^A T_{k+1}^k) \quad \text{Equation 22b}$$

All entities on the right hand side of Equation 22 are known. This allows the calculation of $P(NOM_{j(k+1)})$, which is used in the application of Bayes theorem as per Equation 8. The Bayes network is begun with a known state for a satellite at $k < 0$ and the Markov chain calculation allow the calculations to traverse the network forward. Its result is to produce a vector, denoted as $\mathbb{X}_j$, which contains a sequence of numerical values of $P(NOM_{jk} \mid r_{jk})$ or X_{jk} for all k, both in the prior data and the new data (Figure 3.1). Or, the length of vector $\mathbb{X}_j$ is equal to the running total number of Brightness Data points in the prior data and new data. The belief or marginal probability of the NOM state is the expected value for $P(NOM_{jk} \mid r_{jk})$. Or,

$$Belief\ (NOM_{jk}) = \mathbb{E}_R\big[\,P\,(\,NOM_{jk}\mid R = r_{jk}\,)\,\big] = \mathbb{E}_R\,[\,\mathbb{X}_j\,] \qquad \text{Equation 23}$$

Where $\mathbb{E}_R$ denotes the expected value (i.e. mean) with respect to all values of R. The belief can be computed for the prior data and compared with the new data (see Section 15). Or it can be computed for a moving set of passes (e.g. for a moving block of thirty passes such as from $0 \le k \le 29,\ 1 \le k \le 30$, etc.

10. OUTLIERS AND ANOMALY DETECTION

If the belief changes from the prior data to the new data, it implies anomaly or change in the satellite (see Equation 23). However, the data set corresponding to k ≥ 0 can be very small. For example, in case prior data that spans two weeks, there would be about 30 points of Brightness Data for each of the three regions in Figure 2.2, or the length of vector $\mathbb{X}_j$ for each region of the prior data would also be 30. The new data for X_{jk} for each of the three regions may be collected at a rate of three points per day. Thus, challenge is to identify change in a satellite based on reference data set that has about 30 points and new data that is as small as three points. In such cases, the use of Equation 23 to calculate belief is inadequate. As a result, the anomaly detection is performed using a combination of three types of evidence; namely X_{jk} and two likelihood ratios determined using cluster-based evidence and model-based evidence.

The first evidence is to determine if the X_{jk} for the current pass is an outlier with respect to the prior data for X_{jk}, k < 0. This evaluation is performed separately for the specular and each Lambertian region so that the outliers corresponding to the various anomalies described in Section 5 can be identified. This is described in Section 11. The second evidence is based on the values of X_{jk}^{Peer} in order to identify the ripple effect of the outlier in X_{jk}. This is described in Section 12. The third evidence is to perform model based correction and to re-evaluate X_{jk} to assess if it continues to be an outlier. For example, in case of $CrossTag$, the term I_{mjk} in Equation 2b can be temporarily replaced by the predicted brightness for the cluster peer satellite. This is described in Section 13.

These three sets of evidence are combined and propagated as per the Bayes network. This is described in Section 14. A change in satellite behavior is detected if the evidence of an outlier persists over multiple cycles. In other words, it is an iterative assessment. This calculation can be performed even if the new data comprises very few passes. These calculations are simpler but they do not allow well-quantified hypothesis tests, which are essential in order to generate probabilities of Type I and Type II errors, α and β, which are related to the confidence and power of the test. For example, α is the value of the probability that a satellite would be deemed ANOM when it actually NOM. This is described further in Section 16.

11. USE OF Z-SCORE FOR DETECTION OF OUTLIERS

The rationale for this test is to consider the $(1-X_{jk})$ values for the prior data to be the status quo and examine the $(1-X_{jk})$ for each pass k ≥ 0 in the new data to assess if there has been a change in $(1-X_{jk})$ from the status quo. The status quo is defined through the mean and standard deviation of $(1-X_{jk})$ for passes k < 0 for the prior data. Specifically:

$$\mu_{k<0}^{j} = \mathbb{E}_k[\,(1 - X_{jk})] \qquad\qquad k < 0 \qquad \text{Equation 24}$$

$$\big(\sigma_{k<0}^{j}\big)^{2} = Var\,\big[(1 - X_{jk})\big] \qquad\qquad k < 0 \qquad \text{Equation 25}$$

Where

$\mathbb{E}_k$ denotes the expected value

$\mu^j_{k<0}$ is the mean of (1-X_{jk}) for the prior data, k < 0

$\sigma^j_{k<0}$ is the standard deviation of (1-X_{jk}) for the prior data, k < 0

The first step is to estimate the quantities $\mu^j_{k<0}$ and $\sigma^j_{k<0}$ based on a limited set of X_{jk} values for the prior data. At present, this calculation is performed by assuming that the mean and variance of X_{jk} are constant for all k < 0 but depend on j. These estimates for the mean and variance are denoted as $\bar{x}^j_o$ and s^j_0, respectively.

In order to determine whether or not there has been a change in X_{jk} from the status quo, a basic z-score measure ζ^j_k is defined in the following [Reference 23]. It is useful when only a few observations of new data are available. The magnitude of this z-score is meant to prompt the user to assess if the satellite has changed relative to the status quo. Specifically, the z-score for pass k is given by:

$$\zeta^j_k = \frac{X_{jk} - \bar{x}^j_o}{s^j_0} \qquad \text{Equation 26}$$

The user chooses a threshold level for the magnitude of ζ^j_k, outside of which the satellite is expected to be ANOM. This calculation is performed at each pass k and the result is a time evolution of the z-score based on which a user may make a judgment in regards to a change in a satellite. Note that for this computation, the user can choose to update the values of mean and variance that are used as inputs to the z-score calculation.

Note that the knowledge of z-score evolution over time is useful for a basic assessment of the anomaly type for the generation of a message for use in the Bayes belief propagation. For example, if the z-score outliers are only for the passes corresponding to observation geometry for the specular region, it is likely to be caused by $OffsetChange$. If the outliers occur sporadically within a night, it may be due to repeated occurrences of $CrossTag$. If an outlier only occurs for an isolated data point and then corrects itself, it may be due to a mistag caused by UCT. If the outliers are persistent at all phase angles and possess a structure, it may be due to a 180º yaw $Turn$ of the satellilte. If the outliers are persistent at all phase angles and lack a structure, it may be because the satellite is $Unstable$, etc.

12. CLUSTER BASED SUPPORTING EVIDENCE OF ANOMALY

As illustrated in Figure 2.1, the Brightness Data can be collected for all satellites in a cluster simultaneously. Accordingly, it is assumed that the Brightness Data for the entire cluster is available to the statistical assessment algorithm for each pass (Figure 6.1). Indeed, the statistical assessment will run in a sequence for one satellite in the cluster after another, creating a separate chain of data for each satellite (Figure 12.1a). The calculation of vector $\mathbb{X}_j$ and the z-score values can thus be performed sequentially for each satellite C_j that belongs to the cluster. This is practical because of the sparse rate at which the Brightness Data is collected. The duration of time between passes is expected to be 10x longer than the time required to compute X_{jk} and ζ^j_k values for each satellite in the cluster.

The cluster data for X_{jk} and z-score provides a second opportunity to gather evidence. For example, if the z-score is an outlier for all satellites in the cluster, it may be due to a noisy observation or due to the crossing of a debris field (UCT) in the line of sight of the sensor. If the outliers occur simultaneously for cluster peers, it may be due to $CrossTag$. Such cluster-based evidence is expressed in terms of a likelihood ratio such as:

$$m^{Cluster}_{jk} = \frac{\mathcal{L}\,(CrossTag)}{\mathcal{L}\,(no\ CrossTag)} = \frac{P\left(ANOM_{jk}\mid r_{jk}\right)P\left(ANOM^{Peer}_{jk}\mid r^{Peer}_{jk}\right)}{P\left(NOM_{jk}\mid r_{jk}\right)P\left(NOM^{Peer}_{jk}\mid r^{Peer}_{jk}\right)} \qquad \text{Equation 27a}$$

$$P\left(ANOM_{jk}\mid r_{jk}\right) = 1 - P\left(NOM_{jk}\mid r_{jk}\right) = 1 - X_{jk} \qquad \text{Equation 27b}$$

Where $\mathcal{L}\,(CrossTag)$ is likelihood for the presence of $CrossTag$, and $m^{Cluster}_{jk}$ is the message sent to the GEO status node for satellite C_j pass k. Use of $m^{Cluster}_{jk}$ during the belief propagation is described in Section 14. Note that multiple such messages can be derived from the cluster-based evidence and sent to the GEO status node.
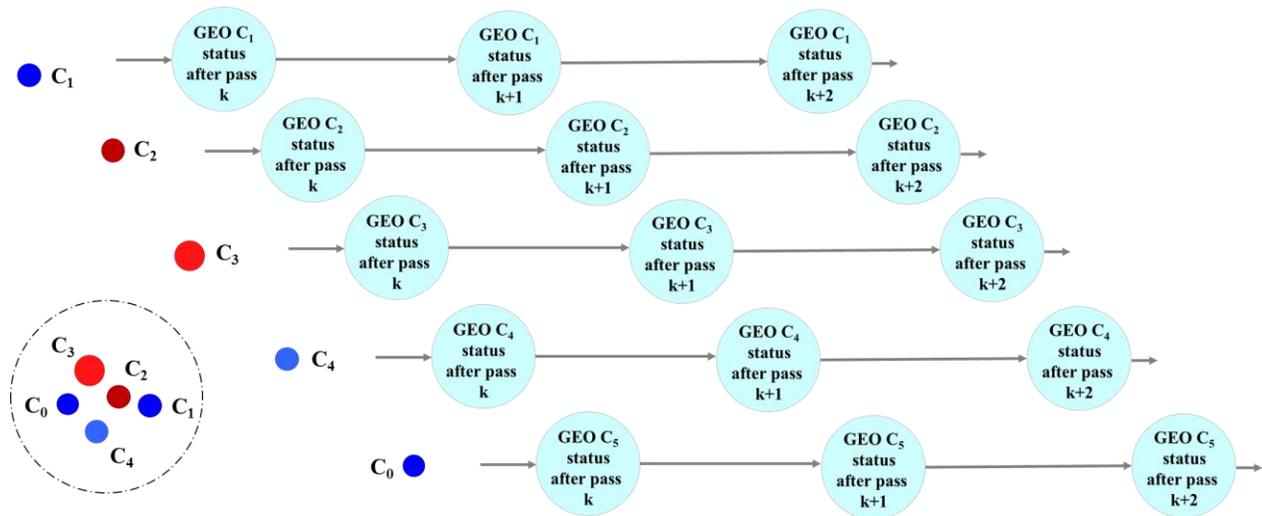
Figure 12.1a: Bayes network for each satellite in the cluster are independent of each other
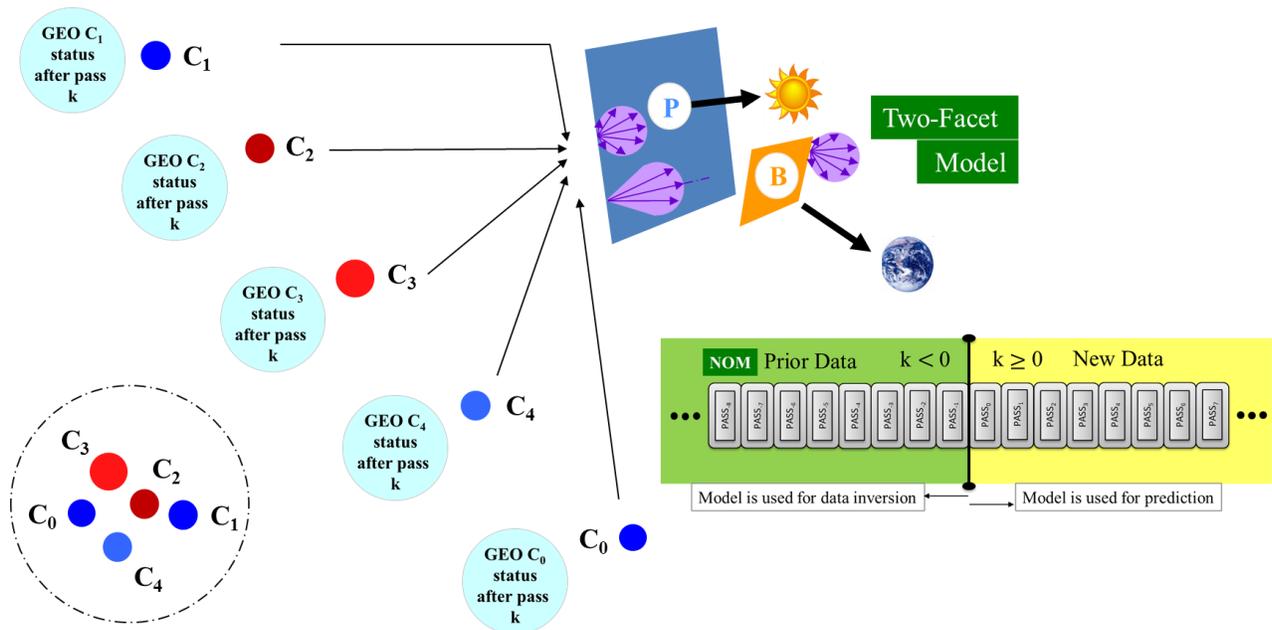
Figure 12.1b: Predictive model can be applied to each satellite in the cluster

13. MODEL BASED SUPPORTING EVIDENCE OF ANOMALY

The present work utilizes the two-facet model to perform inversion of prior data to determine the pose-dependnent body and solar panel albedo-area products for three-axis stabilized GEO satellites (Figure 12.1b). The Brightness prediction for the calculation of r_{jk} is performed by utilizing the previously computed albedo-area products along with the specific observation conditions for pass k in the new data. This calculation is a generic process and it is applied sequentially to each satellite in the cluster. The ability to use the two-facet model on demand provides a third opportunity to gather evidence, which can be communicated back to the GEO status node as a message. This evidence is extracted as a likelihood ratio based on the PDF of the Brightness Ratio as follows:

For example, consider a situation when the cluster based evidence indicates possibility of $CrossTag$ anomaly for satellites C_j and C_j^{peer}. If the $CrossTag$ was true, the Brightness Ratio for the two satellites utilized in the calculation of X_{ij} and X_{ij}^{Peer} have been calculated using incorrect values of v_{jk} and v_{jk}^{Peer} as follows (Equation 2):

For satellite C_j: $\qquad v_{jk} = \dfrac{I_{ojk}}{I_{mjk}^{Peer}}$ $\qquad$ and $\qquad r_{jk} = 1 - v_{jk}$

For satellite C_j^{peer} : $\qquad v_{jk}^{Peer} = \dfrac{I_{ojk}^{Peer}}{I_{mjk}}$ $\qquad$ and $\qquad r_{jk}^{Peer} = 1 - v_{jk}^{Peer}$

The Predictive Model may be used to perform a numerical trial. If there was $CrossTag$, a trial for the resolution of a crosstag can be performed by correcting the values of v_{jk} and v_{jk}^{Peer}. This requires that predicted values of Brightness used in denominator for the calculation of v_{jk} and v_{jk}^{Peer} are switched from satellite C_j to C_j^{peer} and vice versa. Then,

For satellite C_j: $\qquad v_{jk} = \dfrac{I_{ojk}}{I_{mjk}}$ $\qquad$ For satellite C_j^{peer} : $\qquad v_{jk}^{Peer} = \dfrac{I_{ojk}^{Peer}}{I_{mjk}^{Peer}}$

The likelihood ratio for $CrossTag$ may now be computed using the PDF for the corrected values of the Brightness Ratio for the cluster peers as follows:

$$m_{jk}^{Model} = \frac{\mathcal{L} \left(no\ CrossTag\ |\ corrected\ r_{jk}\ and\ r_{jk}^{Peer} \right)}{\mathcal{L} \left(CrossTag\ |\ corrected\ r_{jk}\ and\ r_{jk}^{Peer} \right)}$$

$$= \frac{P \left(corrected\ r_{jk}\ |\ NOM_{jk} \right) P(corrected\ r_{jk}^{Peer}\ |\ NOM_{jk}^{Peer})}{P \left(corrected\ r_{jk}\ |\ ANOM_{jk} \right)\ P(corrected\ r_{jk}^{Peer}\ |\ ANOM_{jk}^{Peer})} \qquad \text{Equation 28}$$

Where m_{jk}^{Model} is the message from the model to the GEO status node for satellite C_j pass k. Use of m_{jk}^{Model} during the belief propagation is described in Section 14. Note that multiple such messages can be derived from the model-based evidence and sent to the GEO status node.

14. BELIEF PROPAGATION

Belief is marginal probability. Accordingly, Equation 23 can be used to determine belief at each GEO status node. However a direct use of Equation 23 requires a minimum of 30 points of new data. In order to be able to assess belief even when the size of new data is small, the procedure described in this section is utilized. It propagates a representative measure of belief by combining the three different values of evidence described in Sections 11-13. Specifically: (1) z-score ζ_k^j for $P(NOM_{jk}\ |\ r_{jk})$, which identifies outliers. These are the passes where $P(ANOM_{jk}\ |\ r_{jk})$ is high ; (2) Message $m_{jk}^{Cluster}$, which is a cluster-based likelihood ratio for $ANOM_{jk}$; (3) Message m_{jk}^{Model}, which is a model-based likelihood ratio for the resolution of $ANOM_{jk}$. Figure 14.1 illustrates a process for the propagation of representative value for belief by combining the three different values of evidence values at each GEO status node as follows [Reference 5]:

$$\mathfrak{B} (ANOM_k) = \zeta_k^j\ m_{jk}^{Cluster}\ m_{jk}^{Model} \qquad \text{Equation 29}$$

Where $\mathfrak{B}$ is a representative measure of belief or score for ANOM at pass k. A user can define threshold values for $\mathfrak{B}$. The values of $\mathfrak{B}$ cross can be monitored in real-time and a warning issued if the threshold is crossed repeatedly.
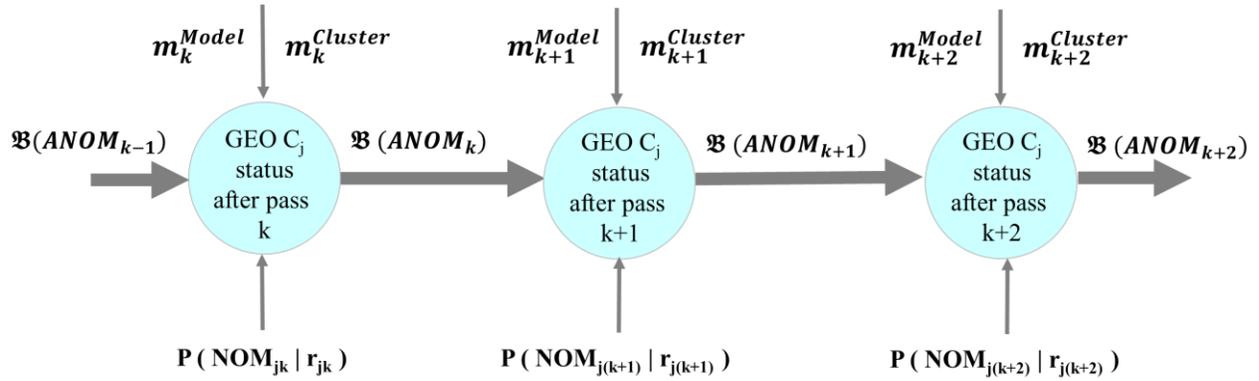
Figure 14.1: Illustration of the belief propagation process [Reference 5]

15. DECISION TO MOVE THE TIME SLIDER

At the root of the mathematics presented in the preceding sections is the prior data, which is used to calculate $f\left(r_{jk} \mid NOM_j \right)$. Since the prior data is for the NOM state, which itself can evolve over time, it is necessary to exercise due diligence prior to denoting that the satellite is NOM for a set of passes (i.e., over an interval of time). It is further necessary that this set comprise at least 30 passes as described in the following.

It is important to attain a balance between the probabilities of false alarm and the probability of missing anomalous behavior in a way that fulfills the user requirements. These two values of probability cannot be obtained using the z-score approach described in Section 11. These two probabilities can be determined by developing suitable hypothesis tests and computing the estimates of Type I and Type II errors [Reference 23]. In order to compute these probabilities, it is necessary to develop certain distributional assumptions in regards to X_{jk} for the prior data (k < 0), and employ a z-score measure for the new data (k≥0) for which a probability distribution can be obtained or approximated. This requires sufficiently large number of points for X_{jk} for the prior data and new data (such as a sample size of 30 or more for each). Upon collecting such data and determining that the satellite behavior is NOM, the time slider can be moved forward to new position up to which the satellite is shown to be NOM.

The calculation of probability distribution for the z-score would be easier if X_{jk} were independent variables. However, this is not likely to be the case as each X_{jk} is computed using input from $X_{j(k-1)}$. Thus, the present problem is, in fact, a part of the eternal statistical conflict between small sample sizes and margin of error.

Section 11 defines the z-score measure ζ_k^j using Equation 26. Its simplicity comes at the expense of not being able to quantify the probabilities of Type I and Type II errors. To this end, a second z-score measure η_k^j is defined as follows [Reference 26]:

$$\eta_k^j = \frac{\bar{X}^j - \mu_{k<0}^j}{\sigma_{k<0}^j / \sqrt{k+1}} \qquad \text{Equation 30}$$

where $\bar{X}^j$ denotes the sample mean of observations $X_{j0},\ldots,X_{jk}$, k ≥0. If the $X_{j0},\ldots,X_{jk}$ were independent and identically distributed, this statistic would have an approximate standard normal distribution for large enough k and could be used as a test statistic for a hypothesis test. This test would allow the calculation of Type I and Type II errors using standard theory. Specifically:

$$H_o: \mu_{k\geq0}^j \text{ is equal to } \mu_{k<0}^j \qquad\qquad H_a: \text{mean } \mu_{k\geq0}^j \text{ is not equal to } \mu_{k<0}^j$$

$$\text{where } \mu_{k\geq0}^j = \mathbb{E}_k[X_{jk,}] \text{ , } k \geq 0 \quad \text{Equation 31}$$

However, the values for $X_{j0},\ldots,X_{jk}$ are not independent. They are more likely to be α-mixing [Reference 26]. The assumption of α-mixing indicates an approximate independence. It is reasonable to assume that the sequence X_{jk} is m-dependent, which is defined as follows:

$(X_{j0}, \ldots, X_{jh})$ is independent of $(X_{jn}, X_{j(n+1)}, \ldots \ldots)$ whenever $n-h > m$, for some integer m and any h.

If so, the α-mixing property follows accordingly. Furthermore, assuming that X_{jk} is stationary (i.e., the joint probability distribution of $(X_{jn}, \ldots, X_{j(n+k)})$ does not depend on n), a Central Limit-type theorem for stationary α-mixing sequences can be employed so that η_k^j has an approximately normal distribution, with $\sigma_{k<0}^j$ replaced by σ^j as follows [Reference 26]:

$$limit_{k \to \infty} \frac{1}{k+1} Var\left(X_{j0} + X_{j1} + X_{j2} + \cdots + X_{jk} \right) = (\sigma^j)^2 \qquad \text{Equation 32a}$$

$$\text{where } (\sigma^j)^2 = \mathbb{E}\left[\left(X_{j0} - \mu_{k \geq 0}^j \right)^2 \right]$$

$$+ 2 \sum_i \mathbb{E}\left[\left(X_{j0} - \mu_{k \geq 0}^j \right)\left(X_{ji} - \mu_{k \geq 0}^j \right) \right] \qquad \text{Equation 32b}$$

Equation 32 is an adjustment of the variance of each X_{ji} to account for the dependence. It is necessary to account for this dependence because it affects the accuracy of Type I and Type II error estimates, compromising the calculation of the probability for the false positives and false negatives.

Since η_k^j is approximately normally distributed for large enough k, the hypothesis is rejected when the observed test statistic value is such that

$$\eta_k^j < -z_{\alpha/2} \text{ or } \eta_k^j > z_{\alpha/2}$$

where $z_{\alpha/2}$ denotes the upper $(100)(\alpha/2)^{th}$ normal percentile. Rejecting the null hypothesis means that the test procedure concludes that the mean of the X_{jk} for passes $k \geq 0$ is different from its value for passes $k < 0$. When the hypothesis test is performed at a significance level α, there is a probability of α that the test procedure will cause the incorrect assertion that the mean X_{jk} for new data $(k > 0)$ is not equal to its estimated mean based on the prior data, $\mu_{k<0}^j$. This is the Type I Error.

To quantify a Type II Error, suppose that the user requirement is to attain at least (1-β) probability that the chosen test procedure correctly rejects the null hypothesis, when the true mean based on the process for passes $k \geq 0$ is not $\mu_{k<0}^j$ but rather it is $\mu_{k<0}^j + \delta$. In this case, it is necessary to consider the sample mean of $(X_{j0} + \ldots + X_{jk})/(k+1)$, where sample size k+1 is at least $(z_{\alpha/2} + z_\beta)^2 \sigma_j^2/(\delta^2)$ [Reference 26]. The justification of this power, as well as the distribution of the test statistic itself, assumes that the estimates of $\mu_{k<0}^j$ and of σ^j are "known" quantities.

There are two drawbacks of this method. First, the test is predicated on full confidence in the estimates $\mu_{k<0}^j$ and $\sigma_{k<0}^j$. The margins of error associated with these estimates play an underlying role in the error rates of the test. Second, estimating $\sigma_{k<0}^j$ is a complex problem related to estimating a covariance matrix of a multivariate distribution and it is difficult to compute when the data set is small. As a practical matter, if the prior data set contains too few observations, this complicates the estimation of $\sigma_{k<0}^j$ and/or increases the margin of error for the estimate. It is anticipated that this situation will lend itself to the bootstrap resampling technique in order to evaluate and quantify confidence in this estimate [Reference 24].

16. NEAR-REAL TIME ASSESSMENT

Figure 16.1 illustrates how the Control Logic in the Statistics Model is posed such that it is feasible to provide a near-real time assessment of NOM or ANOM states for GEO satellites as each new point of Brightness Data is received. The procedure is near-real time in that the assessment can be obtained well in advance of the time when the next data point for Brightness Data is expected to become available. The salient components of the Statistics Model are identified with box numbers in the flow chart. These boxes can be mapped to various figures and equations in the paper, as summarized in Table 16.1. Almost all calculations comprise small computational effort for a desktop computer. The most computationally intensive part of the method is the utilization of the two-facet model for inversion of the prior data (Figure 3.1), taking several minutes per satellite. However, this calculation is required only when the time slider is moved to a new location.

The utilization of a Bayes network for statistical assessment has important collateral benefits as follows. It generates a chronological chain for photometric characterization data for a satellite, which lends itself naturally to a "last-in first-out" type of data archival structure. A chain of such data can be generated for each satellite of interest and then used for its life cycle assessment. Furthermore, the Bayes network structure for photometry-based assessment can be combined with the Bayes network structure for metrics-based assessment in order to create the ability to perform a metric-photometric assessment of satellite status in near-real time[Reference 4].
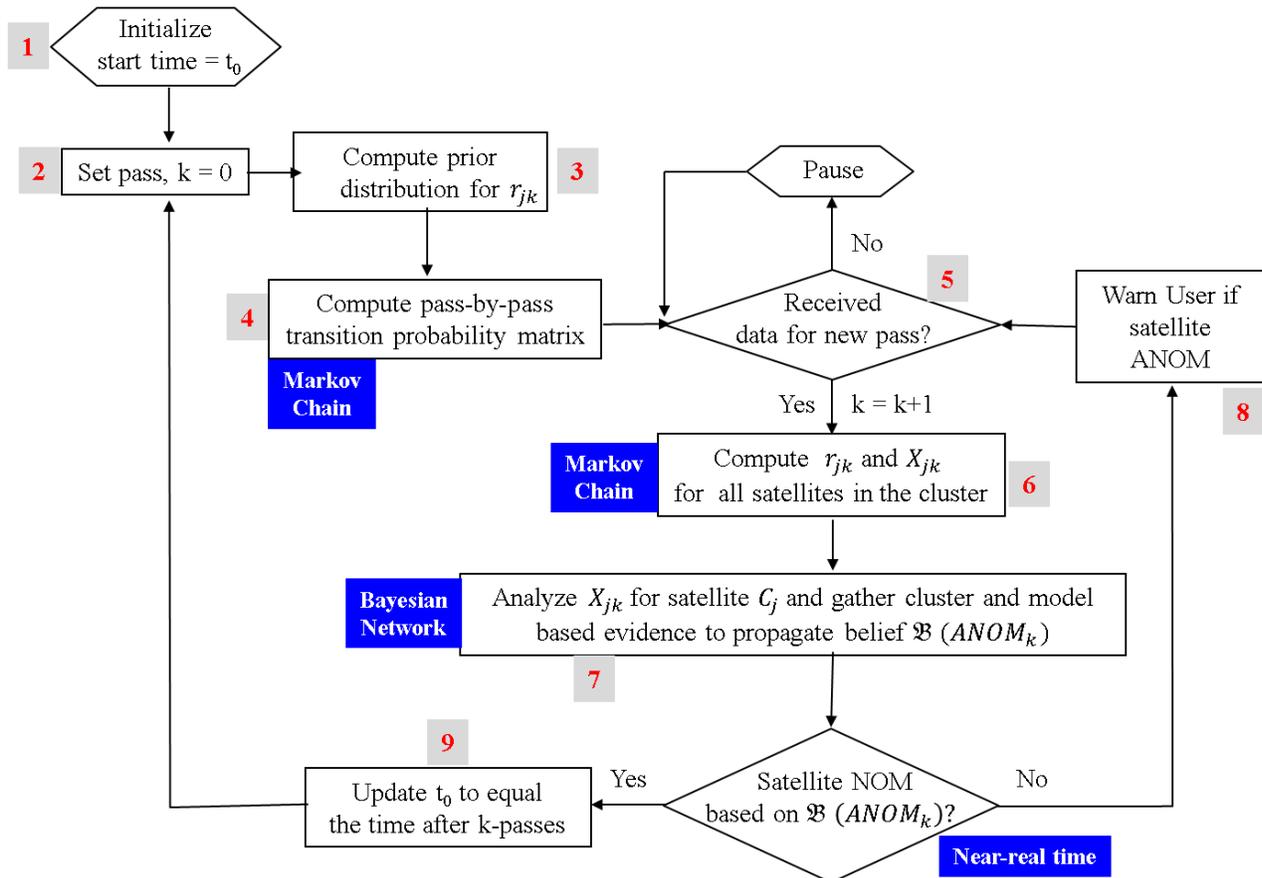
Figure 16.1: Control Logic in the Statistics Model

Table 16.1: Mapping of the flow-chart boxes to technical description

Box	Title	Mapping to the technical description
1	Initialize t_0	Section 3, Timer slide definition
2	Set pass k = 0	Figure 3.1: Prior data for k < 0. New data for k ≥0
3	Compute prior distribution	Sections 5 and 7: PDF for NOM and ANOM
4	Compute transition probability	Section 8: Chapman-Kolmogorov equation
5	Receive data for new pass	Section 2: Character of Brightness Data
6	Compute $P(NOM_k \mid r_k)$	Sections 6,7 and 9: Bayes network, Bayes theorem and Markov Chain
7	Determine belief	Sections 10-13: Outlier detection, z-score, cluster and model evidence
8	Notify user	Section 14: Propagate belief and notify user
8	Update t_0	Section 15, Movement of the time slider

17. ONGOING WORK AND CLOSURE

In light of the formulation for belief propagation and anomaly detection described in the preceding sections, future work entails computing the probabilities of Type I and Type II errors in light of the unavoidable small sample sizes. Even if a large enough training set of prior data exists for belief in satellite status, the user does not want to wait for a large number of passes in order to assess whether the satellite has changed from a NOM state.

To this end, the future work will attempt to address this problem in the context by exploring how the margin of error can be mitigated in two ways. First, bootstrap analysis will be used to improve the estimate of distributional properties of test statistics (η_k^j). Once the distributional properties are established, the calculation for the margin of error can be improved in order to provide the user with the critical values associated with rejecting steady-state.

The use of an alternate functional (i.e., a function whose domain is a set of functions) with more desirable statistical properties will be explored in order to represent the belief process. Here "more desirable" means that the distributional properties of a test statistic derived from this functional can be calculated within the constraints of the current problem of anomaly detection. For example, such a statistic may exploit potential independence of increments (such as $X_{jk} - X_{j(k+1)}$), independence of time blocks (such as belief gathered at non-overlapping time frames), or other measures of stability (e.g., sample median).

The distribution of the belief process in the larger context of stochastic processes will be explored. Statistical analysis involving model fitting is the first step toward this goal, including autoregressive or other mean reverting models. Software already exists to obtain parameter estimates for such processes, and as such a comparison of estimated parameters in the prior with those of new data could lend itself to improvement in the definition of the PDF for prior and new data and an additional test for change in belief in the status of a satellite.

18. ACKNOWLEDGEMENT

19. REFERENCES

1   Chaudhary, A.B., Payne, T.E., Lucas, K., Mutschler, S., Vincent, T., Dao, P., and Murray-Krezan, J., "Point Pairing Method Based on the Principle of Material Frame Indifference for the Characterization of Unknown Space Objects using Non-Resolved Photometry Data", AMOS 2013 Technical Conference, Maui, HI.
2   Payne, T. E, Lucas, K., Chaudhary, A.B., Mutschler, S., Dao, P., Murray-Krezan, J., "A Derivation of the Analytical Relationship between the Projected Albedo-Area Product of a Space Object and its Aggregate Photometric Measurements", AMOS 2013 Technical Conference, Maui, HI.
3   Chaudhary, A.B., Payne, T.E., Gregory, S., Dao, P., "Fingerprinting of non-resolved three-axis stabilized space objects using a two-facet analytical model", AMOS 2011 Technical Conference, Maui, HI.

4   Abbot, R.I., and Wallace, T.P., "Decision Support in Space Situational Awareness", Lincoln Laboratory Journal, Vol. 16, No.2, 2007

5   Yedidia, J.S., Freeman, W.T. and Weiss, Y., "Understanding Belief Propagation and its Generalizations", at http://www.merl.com/publications/docs/TR2001-22.pdf

6   "Marginal distribution", at http://en.wikipedia.org/wiki/Marginal_distribution

7   Payne, T.E., Gregory, S.A., Tombasco, J., Luu, K., and Durr, L., "Satellite Monitoring, Change Detection, and Characterization using Non-resolved Electro-optical data from Small Aperture Telescope", AMOS 2007 Technical Conference, Maui, HI.

8   Payne, T.E., Gregory, S.A., Luu, K., "SSA Analysis of GEO Photometric Signature Classification and Solar Panel Offsets", AMOS 2006 Technical Conference, Maui, HI.

9   Levan, P., "Closely-spaced Objects and Mathematical Groups combined with a Robust Observational Method", AMOS 2009 Technical Conference, Maui, HI.

10   Wallace, B., Scott, R., Spaans, A., "The DRDC Ottawa Space Surveillance Observatory", AMOS 2007 Technical Conference, Maui, HI.

11   Scott, R., and Wallace, B., "Satellite Characterization using Small Aperture Instruments at DRDC Ottawa", AMOS 2008 Technical Conference, Maui, HI.

12   Scott, R., Wallace, B., "Small Aperture Telescope Observations of Co-located Geostationary Satellites", AMOS 2009 Technical Conference, Maui, HI.

13   Ryan E.V., and Ryan, W. H., "The Magdalena Ridge Observatory's 2.4 meter Telescope: A New Facility fir Follow-up and Characterization of Near-Earth Objects", AMOS 2008 Technical Conference, Maui, HI.,

14   Standard score, http://en.wikipedia.org/wiki/Standard_score

15   Markov chain, en.wikipedia.org/wiki/Markov_chain

16   Examples of Markov chains, http://en.wikipedia.org/wiki/Examples_of_Markov_chains

17   Ross, S., "Introduction to Probability Models", Elsevier, 2010, ISBN: 978-0-12-375686-2.

18   Strang, G., "Introduction to Applied Mathematics", Wellesley-Cambridge Press, 1986, ISBN: 978-0961408800.

19   Cayley-Hamilton theorem, http://www.math.colostate.edu/~yzhou/course/math561_spring2011/CHthm.pdf

20   Eigenvalues and eigenvectors, http://en.wikipedia.org/wiki/Eigenvalues_and_eigenvectors

21   Knill, O., "Math 19b: Linear algebra with probability", at http://www.math.harvard.edu/~knill/teaching/math19b_2011/handouts/math19b_2011.pdf

22   Invariants of tensors, http://en.wikipedia.org/wiki/Invariants_of_tensors

23   Walpole, R.E., Myers, R.H., Myers, S.L., Ye, K., "Probability and Statistics for Engineers and Scientists", Prentice Hall, 2007, ISBN: 0-13-187711-9

24   Singh, K., and Xie, M., "Bootstrap: A Statistical Method", www.stat.rutgers.edu/~mxie/rcpapers/bootstrap.pdf , Rutgers University

25. Applied Optimization, Inc., "RADtool: RSO Albedo-area Determination tool", a software application for SSA, 2014.

26. Billingsley, P., "Probability and Measure", John Wiley and Sons, ISBN: 978-1118122372

27. Malvern, L.E., "Introduction to the mechanics of continuous medium", Library of congress catalog card number: 69-13712, Prentice-Hall, 1969, page 7.

28. Dentamaro, T., Boston College, Personal communication, 2013-14.

29. Deiotte, R., Guyote, M., Kelecy, T., Hall, D., Africano, J., and Kervin, P., "Maui Space Surveillance System Satellite Categorization Laboratory", AMOS Technical Conference, Maui, HI 2006

30. Murray-Krezan, J., Inbody, W.C., Dao, P., Dentamaro, A., Fulcoly, D., and Gregory, S.A., "Algorithms for Automated Characterization of Three-Axis Stabilized GEOs using Non-Resolved Optical Observations"AMOS Techical Conference, 2012.

APPENDIX A: NOTATION

Text notation:

Brightness: Value of Brightness Data at a single data point

Brightness Data: Single point brightness data point collected by a ground or space-based sensor during the routine synoptic search operation. This data is collected along with the angles only metric data

Brightness Ratio: Ratio of observed Brightness to predicted Brightness

Body: Body of a GEO satellite

Change: Modification of state of a satellite from NOM to ANOM or vice versa.

Change Detection: To recognize that the state of satellite has undergone Change

Cluster Peer: A pair of satellite in a cluster can be cross-tagged

Inter-pass Time: Temporal spacing between successive orbital passes

NOM: Nominal status of a satellite. This is when the correlation coefficient between the observed Brightness and the predicted Brightness exceeds a user-defined threshold limit.

ANOM: Anomalous status of a satellite. This is when the correlation coefficient between the observed Brightness and the predicted Brightness is below the user-defined threshold limit for NOM.

Panel: Panel term for a GEO satellite (it combines the effect of both solar panels into a single term)

PDF: Probability distribution function

Signature Data: A sequence of Brightness measurements collected by a dedicated sensor during a single pass for a target satellite. For GEO satellites, such data is collected at a frame rate such as one data point per minute, etc.

Mathematics notation:

$\mathfrak{B}$ is a representative measure of belief or a score for ANOM at pass k

C_j = jth satellite in a GEO cluster

$\mathfrak{L}(CrossTag)$ is likelihood for the presence of $CrossTag$

$\mathbb{E}_k$ denotes the expected value

$\mathbb{E}_R$ denotes the expected value (i.e. mean) with respect to all values of R

$\mathbb{E}_Y$ = Expected value or mean for a quantity irrespective of y

$f(r_{jk})$ is the PDF for the Brightness Ratio for pass k for satellite C_j

$f(r_{jk} | ANOM_j)$ is the PDF for the Brightness for pass k Ratio given the satellite C_j is ANOM

$f(r_{jk} | CrossTag_j)$ is the PDF of Brightness Ratio when C_j is cross-tagged with a peer

$f(r_{jk} | NOM_j)$ is the PDF for the Brightness Ratio for pass k given the satellite C_j is NOM,

$f(r_{jk} | OffsetChange_j)$ is the PDF of Brightness Ratio when the C_j panel offset is modified

$f(r_{jk} | Turn_j)$ is the PDF of Brightness Ratio when C_j is turned 180º

$f(r_{jk} | UCT_j)$ is the PDF of Brightness Ratio when mistag is caused by an unexpected UCT

$f(r_{jk} | Unstable_j)$ is the PDF of Brightness Ratio when Cj is unstable

I_{mjk} is the Brightness predicted by the model for satellite j and pass k

I_{ojk} is observed brightness for satellite j and pass k

j is the index for satellite number in a GEO cluster

$\sigma^j_{k<0}$ or s_0 is the standard deviation of X_{jk} for the prior data, k < 0

ζ^j_k is standard z-score for anomaly detection

η^j_k is another z-score measure utilized to forward the time slider

k = Index for an orbital pass number. The time slider origin is k = 0. Prior data is for k < 0. New data is for k ≥ 0.

$m^{Cluster}_{jk}$ message based on cluster based evidence

m^{Model}_{jk} message based on model based evidence

$\mathfrak{L}(CrossTag)$ is likelihood for the presence of $CrossTag$

π_N The long run probability that a satellite is NOM at any time

$P(Crosstag_j)$ is the long run probability of cross-tag for C_j

$P(ANOM_j)$ is the long run probability that the satellite is ANOM, also denoted as π_A; $P(ANOM_j) = 1 - \pi_N$

$P(NOM_j)$ is the long run probability that the satellite is NOM, denoted as π_N, and

$P\left(NOM_{kj} \mid r_{kj}\right)$ = Probability that satellite Ci is NOM after pass k given the Brightness Ratio r_{kj}

$P(OffsetChange_j)$ is the long run probability of change in the panel offset angle for satellite C_j

$P\left(Turn_j\right)$ is the long run probability of a 180° turn for C_j

$P\left(UCT_j\right)$ is the long run probability of mistag for C_j due to the appearance of UCT in the sensor FOV

$P\left(Unstable_j\right)$ is the long run probability that satellite C_j is unstable

$P(X = x)$ = Probability that an outcome for a random variable X equals x

$P(X = x \mid Y = y)$ = Conditional probability for $X = x$ given $Y = y$

r_{jk} = Ratio of observed Brightness of satellite j and pass k to predicted Brightness of satellite j and pass k. This ratio is defined only at the orbital location when Brightness data is collected

$\mathbb{T}$ is the pass-to-pass transition probability matrix

${}_{A}^{A}T_{k+1}^{k} = 1 - {}_{N}^{A}T_{k+1}^{k}; {}_{A}^{A}T$ is the probability of persistence of ANOM over a unit interval of time

${}_{N}^{A}T_{k+1}^{k}$ is the probability of transition of ANOM to NOM over a unit interval of time

${}_{A}^{N}T_{k+1}^{k}$ is the probability of transition of NOM to ANOM over a unit interval of time

Δt_{Gap} is the daytime gap

Δt_k is the temporal spacing between pass k and pass (k+1)

$\mu_{k<0}^{j}$ is the mean of X_{jk} for the prior data, $k < 0$

$v_{jk} = \frac{I_{ojk}}{I_{mjk}}$ is the ratio of observed to modeled brightness at pass k

$\mathbb{X}_j$ is the vector of X_{jk}

$X_{jk} = P\left(NOM_{jk} \mid r_{jk}\right)$

$\bar{X}_{k}^{j}$ denotes the sample mean of observations $X_{j1},\ldots,X_{jk},$ k $\geq 0.$ If the $X_{j1},\ldots,X_{jk}$

$\sum_y$ = Summation over all permissible values of y

$z_{\alpha/2}$ denotes the $(100)(\alpha/2)^{th}$ normal percentile

APPENDIX B: NUMERICAL EXAMPLE: CROSSTAG DETECTION

This numerical example considers the scenario for cross-tag detection in a notional GEO cluster consisting of a pair of cluster peers, C1 and C2. The Brightness Data for satellites C1 and C2 was generated using a numerical simulation performed by the Optical Signatures Code [Reference 28]. The simulation data emulated one data point per pass where the mean gap between the passes was one hour. There was no daytime data. The simulation data was considered for a period of two weeks. The first week of data was treated as prior data and the second week as the new data. Two cases were considered for the simulations as shown in Table B1.

Table B1: Two cases of numerical simulation for CrossTag analysis

Case		Satellite C1	Satellite C2
1	Week 1	NOM	NOM
1	Week 2	NOM	NOM
2	Week 1	Same as Case 1	Same as Case 1
2	Week 2	CrossTag	CrossTag

The prior data was assumed to be available at all times and the new data was assumed to become available as one Brightness Data point at a point. The belief calculation was performed each time a new Brightness Data point is received. The calculations were performed using the two-facet model as the Photometry Model, the Bayes network and the control logic as illustrated in Figure 16.1 [Reference 25]. The Statistics Model was implemented such that the Control Logic can call any analysis procedure on an as-needed basis. The results are reported in Figures B1 to B7. Table B2 provides a key to how the figures are organized. The various different results shown in the figures B1 to B7 correspond to the Boxes in Figure 16.1. Note that each underlying calculations is a discrete step, simple for a desktop computer to execute. Each step was implemented in reusable software modules and the sequence of steps was automatically executed by the Control Logic [Reference 25]. The specifics of each step performed in order to generate Figures B1 to B7 are given after Table B2.

\

Table B2: Organization key for the results in Figures B1 to B7
Week 1 is prior data and Week 2 is new data

Figure	Satellite	Cases	Week
B1a	C1	1 and 2	1
B1b	C1	1 and 2	1
B2a	C2	1 and 2	1
B2b	C2	1 and 2	1
B3a	C1	1 and 2	1
B3b	C1	1 and 2	1
B4a	C2	1 and 2	1
B4b	C2	1 and 2	1
B5a	C1	1 and 2	1
B5b	C1	1 and 2	1
B6a	C2	1 and 2	1
B6b	C2	1 and 2	1
B7a	C1	1	2
B7b	C1	2	2
B7c	C1	2	2

- Figure B1a shows a plot of Brightness data versus time for satellite C1. This is prior data that spans eight days. The last data point in this prior data corresponds to pass k = -1. The observed and modeled Brightness Data is shown in Figure B1b for satellite C1 as function of the orbit angle. The modeled data consists of individual contributions of the Body and the Panels to the satellite signature. The orbit angle is defined in a manner similar to the longitudinal phase angle, except that the phase angle is calculated with respect to the equatorial plane and the orbit angle is computed with respect to the orbital plane of a satellite. Note that the Figure B1b is for the NOM state of the satellite. Figure B2a and B2b show the corresponding calculations for satellite C2.

- The prior data is utilized to compute the prior probability distribution for r_{jk} under NOM conditions. This calculation is performed using Equation 2. It corresponds to Box 3 in the Control Logic shown in Figure 16.1 for satellite C1. The prior distribution is extracted from the histogram and its Gaussian fit shown in Figures B3a and B4a, respectively for satellites C1 and C2.

- The ANOM condition is assumed to only comprise the CrossTag. Or, the only term in the right hand size of Equation 4 is assumed to be due to CrossTag. Equation 10 is utilized to determine the prior probability distribution under ANOM conditions. This distribution is also extracted from the histogram shown in Figures B3b and B4b for the cluster peers C1 and C2. The histograms are quite different for the NOM and ANOM conditions even though the visual magnitudes for the two satellites are quite comparable to each other. This is because of the specific character of the satellite Brightness as a function of phase angle and it is different for the two peer satellites. The NOM distribution is similar to a Gaussian distribution, however it has longer tails. The ANOM distribution is unlike a Gaussian distribution. Note that this character of the NOM and ANOM distribution also depends on the accuracy of the Photometry Model, which varies from one satellite to another. Nonetheless, this difference in the NOM and ANOM distributions is a key to the Statistics Model.

- The value of long run probability for NOM, π_N is assumed to be 0.90 for each satellite. The terminator-to-terminator NOM-to-NOM transition probability is assumed to be 0.95. The transition probability matrix for the daytime gap is computed using Equation 21. The pass-to-pass transition probability matrix is computed using Equation 17b. This is Box 4 in the Control Logic.

- Figures B5 considers two situations for satellite C1 and Figure B6 considers the corresponding two situations for satellite C2. Figure B5a shows a plot of r_{jk} versus orbit angle for satellite C1 if it was correctly tagged in the new data (i.e. the second week of Brightness Data). Figure B5b shows a plot of r_{jk} versus orbit angle if the satellite C1 was cross-tagged with satellite C2 in the new data. Figure B6a shows the plot when satellite C2 was

correctly tagged in the new data and Figure B6b when it was cross-tagged in the new data. The calculations for the ANOM histogram are performed using Equation 10.

- Figure B7a considers the case when satellite C1 was correctly tagged. It shows four graphs. The x-axis is the orbital pass number, or k. The blue graph is a plot of r_{jk}. Note the peaks in the values of r_{jk}, which can be real or due to limitations of the Photometry Model. The red line is the plot of $P(r_{jk} | NOM_{jk})$, which is obtained from the PDF derived from the histogram shown in Figure B3a. The green line is the plot of $P(r_{jk} | ANOM_{jk})$, which is obtained from the PDF derived from the histogram shown in Figure B3b. The purple line is the plot of $P(NOM_{jk} | r_{jk})$, which is obtained using the Bayes theorem. The values of $P(r_{jk} | NOM_{jk})$ are close to one for much of the time. This is expected since the satellite C1 was correctly tagged in this case. Towards the end, there is a drop due to a consecutive set of values of r_{jk} for which $P(r_{jk} | NOM_{jk})$ is low. This is Box 6 in the Control Logic flow chart in Figure 16.1. The persistently high value of $P(r_{jk} | NOM_{jk})$ may be utilized by a user as indicator for correct tagging of a satellite.

- Figure B7b considers the same calculations, except for the case when satellite C1 was cross-tagged. The purple line plot for $P(NOM_{jk} | r_{jk})$ includes large segments where the probability of NOM is close to zero. This may be considered an indicator by the user for the presence of CrossTag anomaly.

- Figure B7c considers the calculations performed for the z-score for $P(ANOM_{jk} | r_{jk})$, the cluster-based evidence $m_{jk}^{Cluster}$, the model-based evidence m_{jk}^{Model}, and the belief $\mathfrak{B}(ANOM_k)$ for CrossTag. This is calculated as per Equation 29. The numerical values $m_{jk}^{Cluster}$ and m_{jk}^{Model} are not allowed to become larger than a threshold value (e.g. 10) in order to prevent one message from overwhelming the other. The propagated belief $\mathfrak{B}(ANOM_k)$ shows a significant regime for ANOM, which may be utilized by a user as indicator for the of ANOM conditions. This is Box 8 in Figure 16.1. Figure B7c shows a notional red line, which is meant to denote a user defined threshold for the presence of CrossTag.

- Note that the $\mathfrak{B}(ANOM_k)$ drop significantly after several passes (Figure B7c). This is in conflict with the high values of belief computed for the balance of the passes. This occurs because the Cross-tagged satellites are equally bright, which is makes it difficult to distinguish between them on the basis of their Brightness.

- If the level of belief for NOM in the new data is on the same level as the prior data and it exceeds a user-defined threshold, the time slider is shifted forward to pass k. This is Box 9 in the Control Logic.

Note that Figures B1 to B6 represent the calculations performed on the prior data. These calculations need to be performed each time the time slider is advanced (Section 15). It takes several minutes of computations in order to perform these calculations. Majority of this time is consumed by the Inversion Model. Figure B7 calculations would be performed each time a new point of Brightness Data is received. These calculations take only a few seconds to complete and thus the evolving belief in NOM or ANOM status can be obtained in near real time.

This example considered an idealized scenario where the cluster comprised only two satellites and the only anomaly could occur was CrossTag. In a more realistic scenario, the cluster may contain more satellites and all anomalies are possible. The calculations necessary to analyze such a scenario consist of many more of that shown in Figure B7. Figures B1 to B6 are for the prior data and they are common to all ANOM assessments.

A salient next step is to synthesize the evolving belief automatically in order to rank the potential ANOM situation.
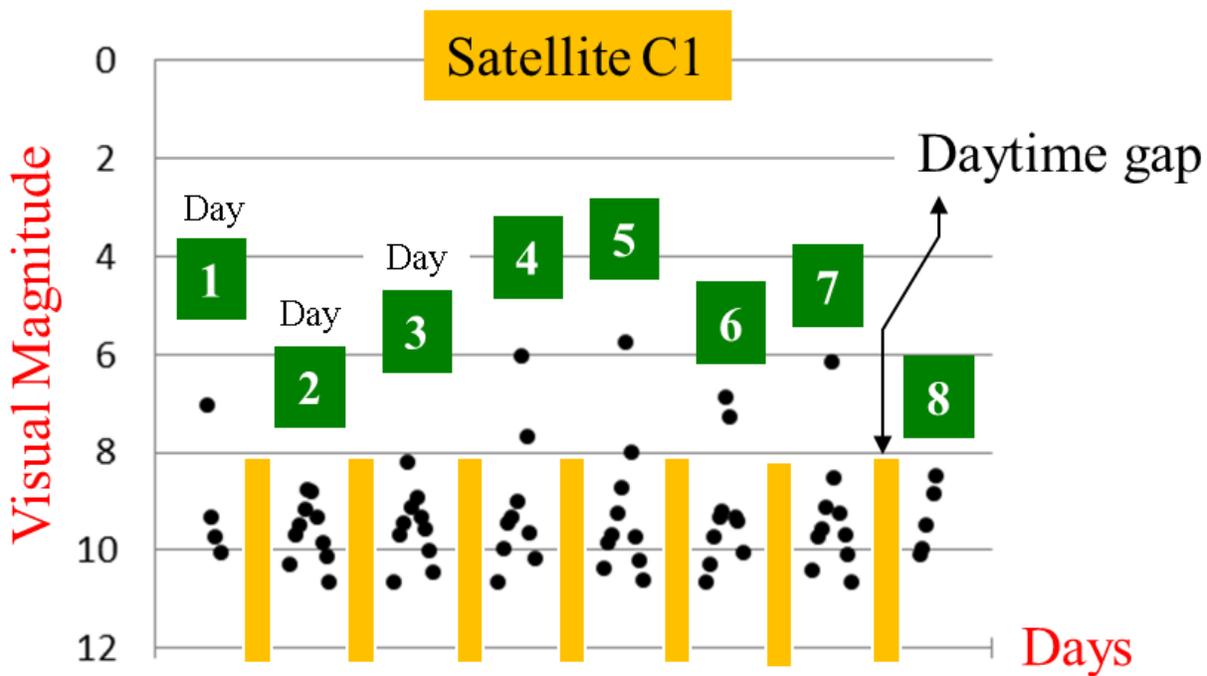
Figure B1a: Brightness Data vs. Time for satellite C1 (prior data)
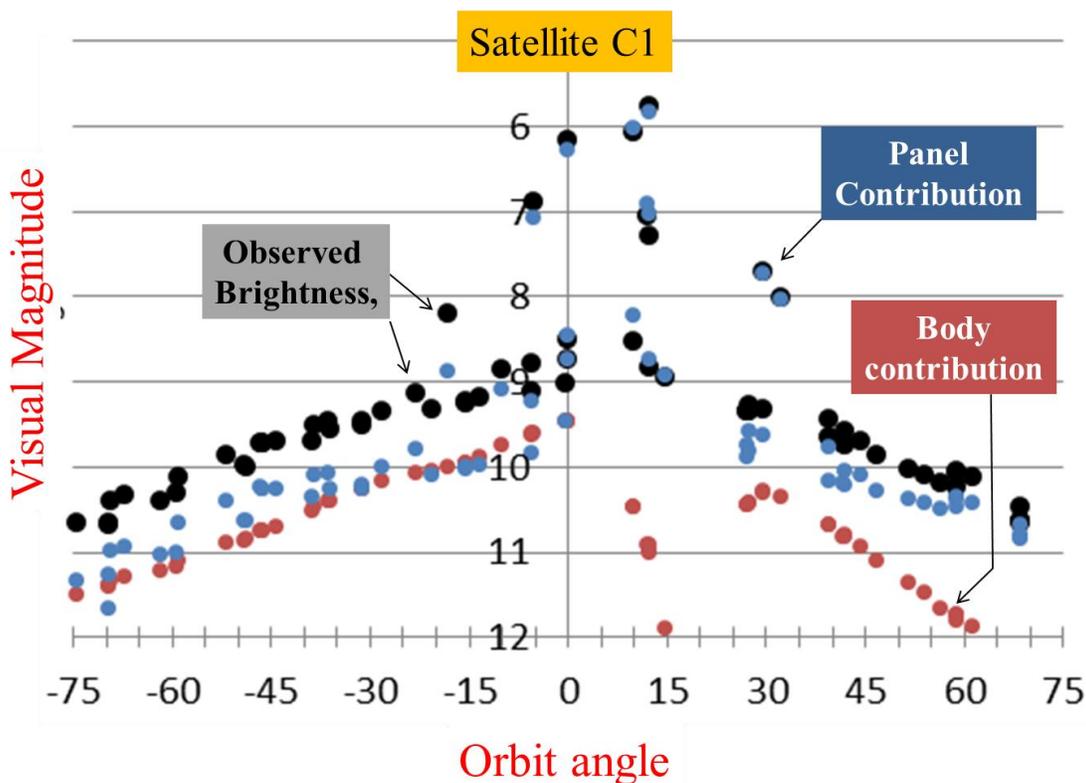
Figure B1b: Observed and Predicted (Modeled) Brightness Data for Satellite C1
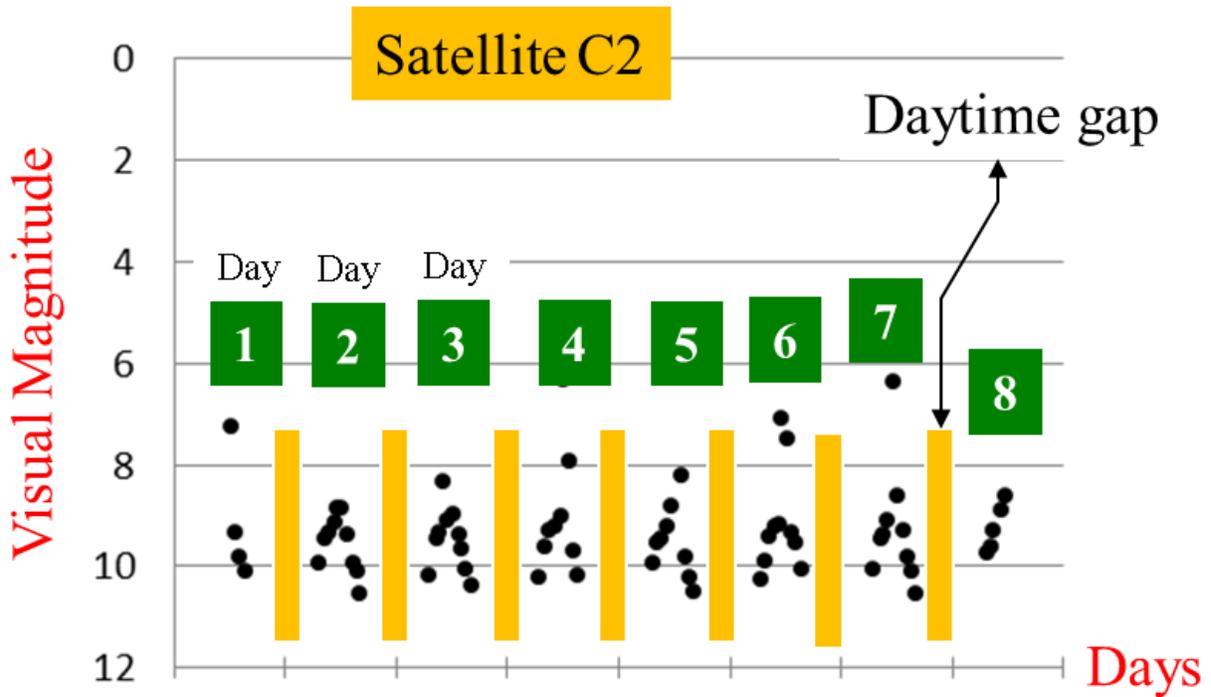
Figure B2a: Brightness Data vs. Time for satellite C2 (prior data)
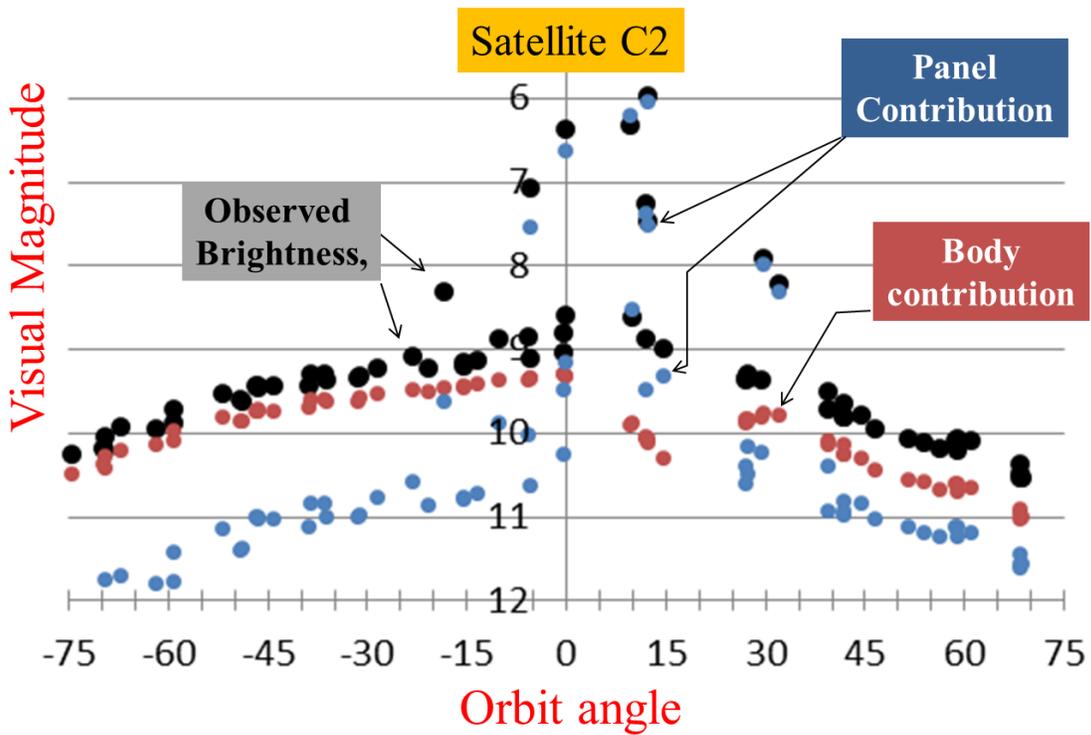
Figure B2b: Observed and Predicted (Modeled) Brightness Data for Satellite C2
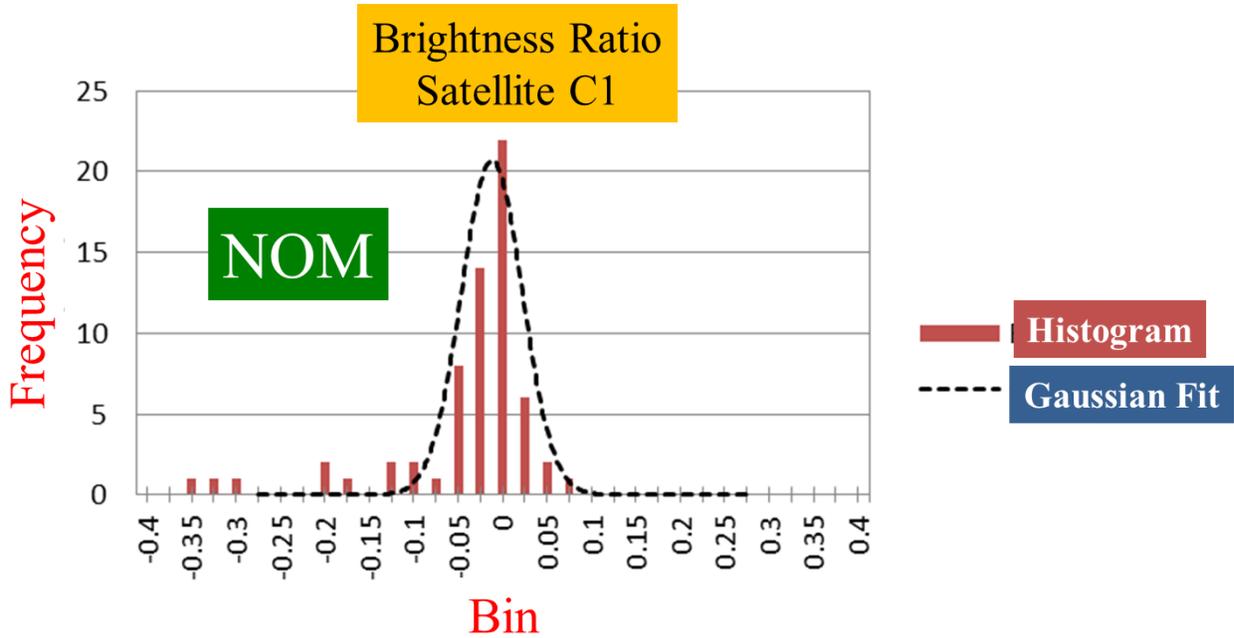
Figure B3a: Prior distribution $f\left(r_{jk} \mid NOM_j\right)$ for satellite C1
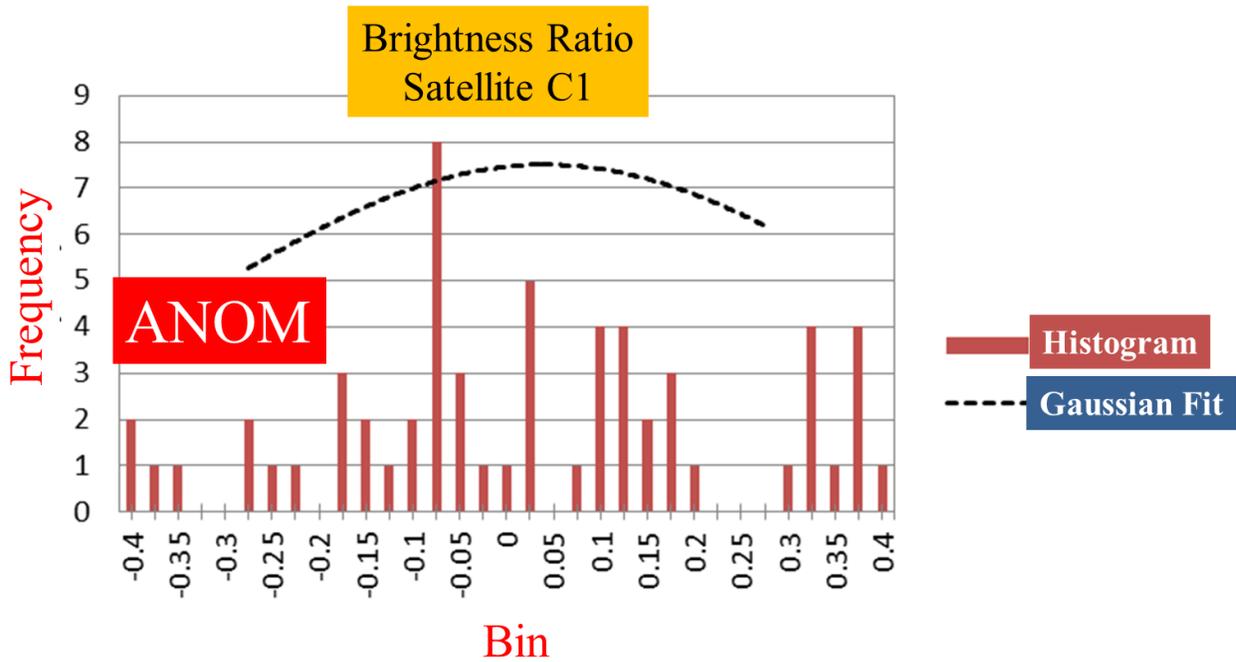
Figure B3b: Prior distribution $f\left(r_{jk} \mid ANOM_j\right)$ for satellite C1
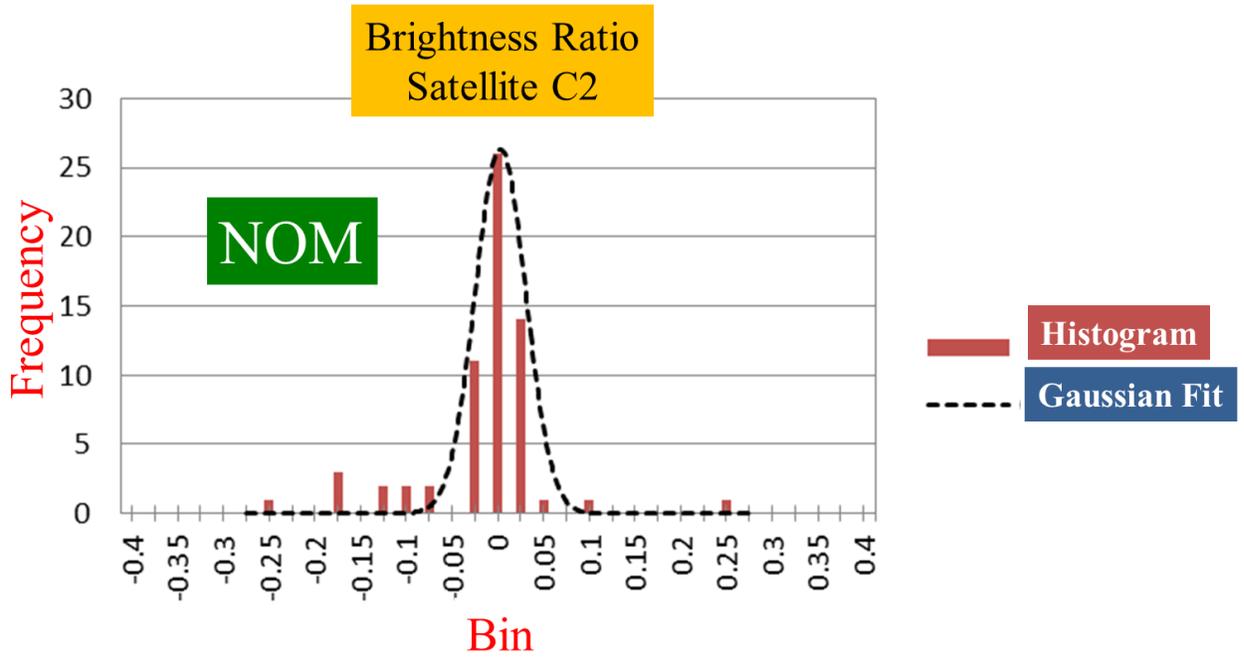
Figure B4a: Prior distribution $f\left(r_{jk} \mid NOM_j\right)$ for satellite C2
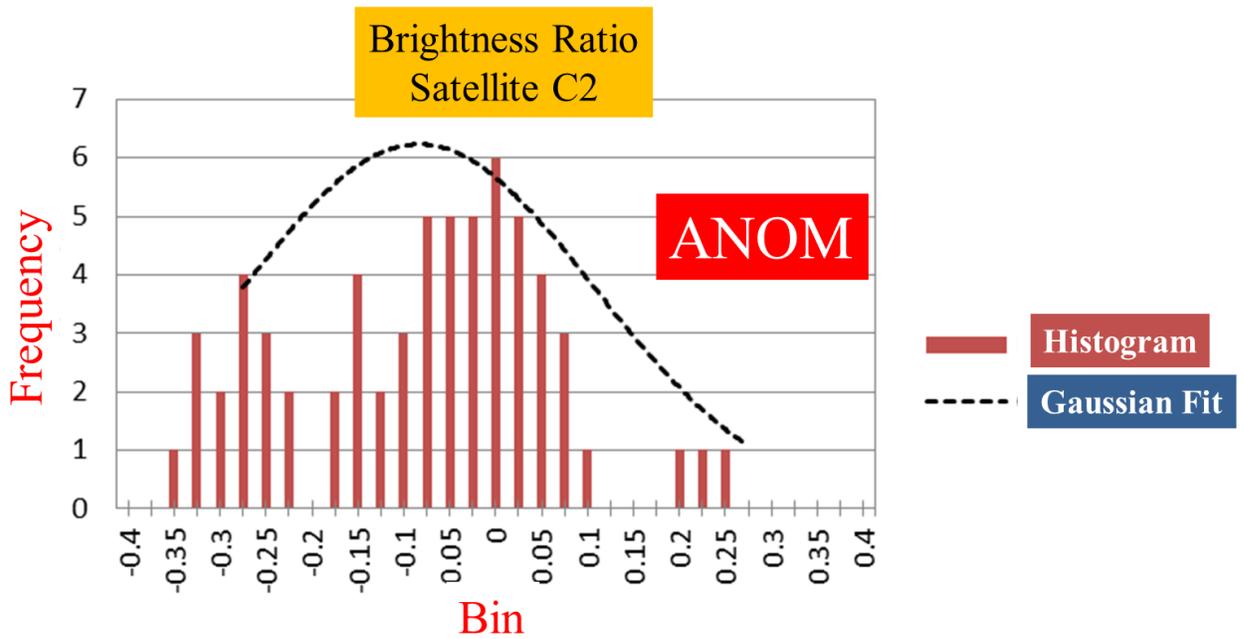
Figure B4b: Prior distribution $f\left(r_{jk} \mid ANOM_j\right)$ for satellite C2
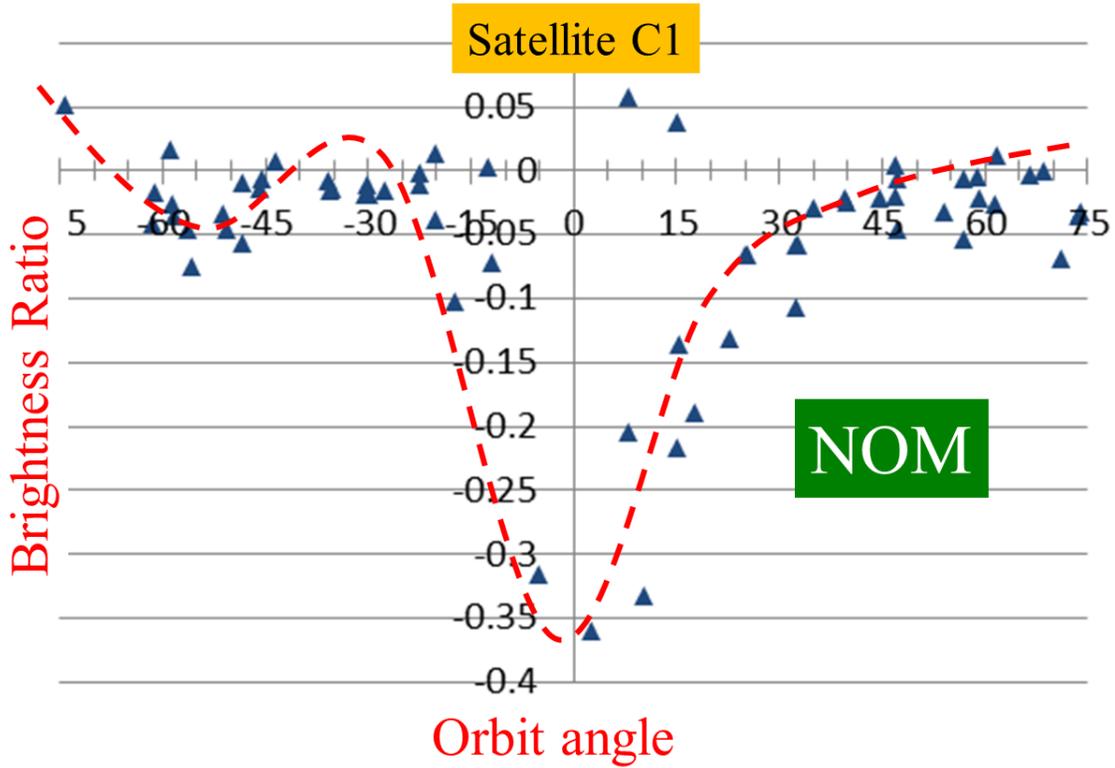
Figure B5a: Plot of r_{jk} for new data (k ≥ 0) versus orbit angle for satellite C1 (NOM)
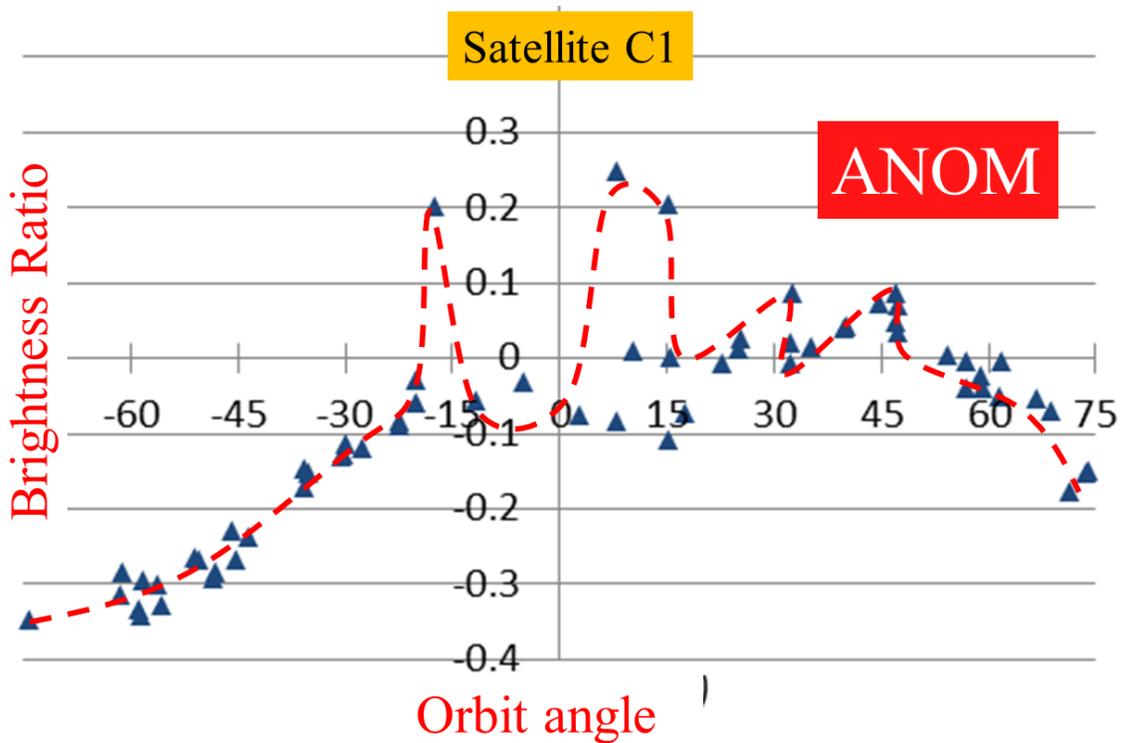
Figure B5b: Plot of r_{jk} for new data (k ≥ 0) versus orbit angle for satellite C1 (ANOM)
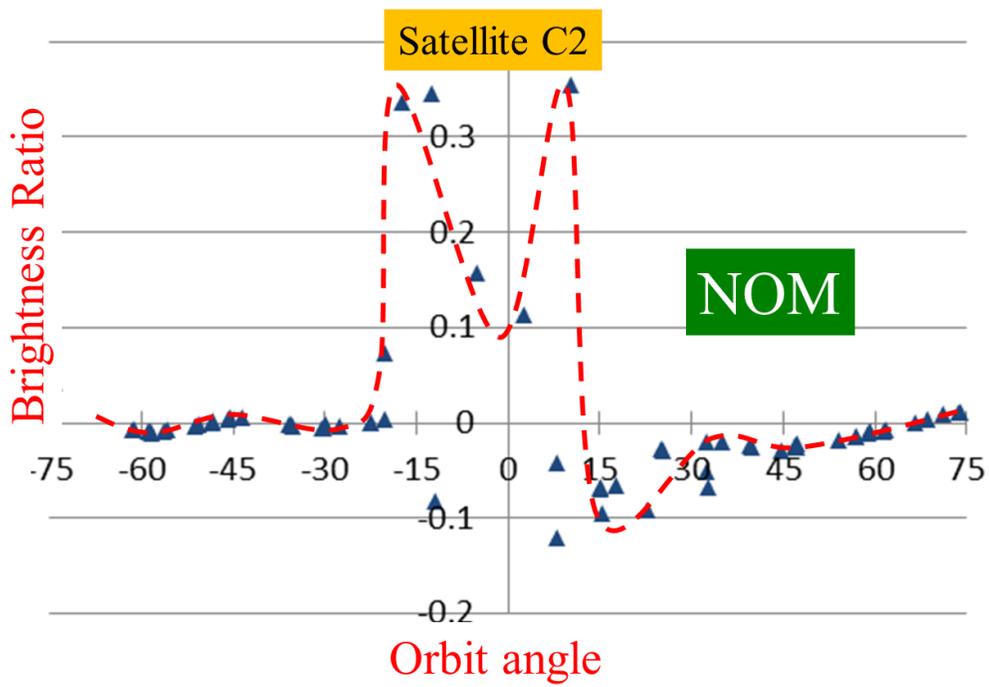
Figure B6a: Plot of r_{jk} for new data (k ≥ 0) versus orbit angle for satellite C2 (NOM)
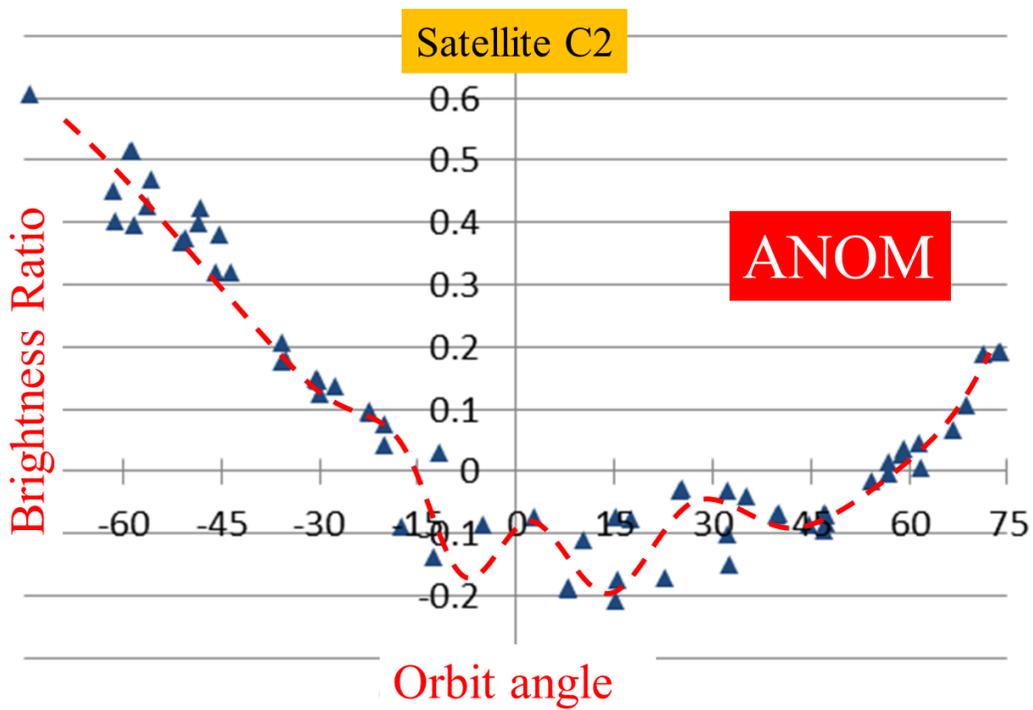
Figure B6b: Plot of r_{jk} for new data (k ≥ 0) versus orbit angle for satellite C2 (ANOM)
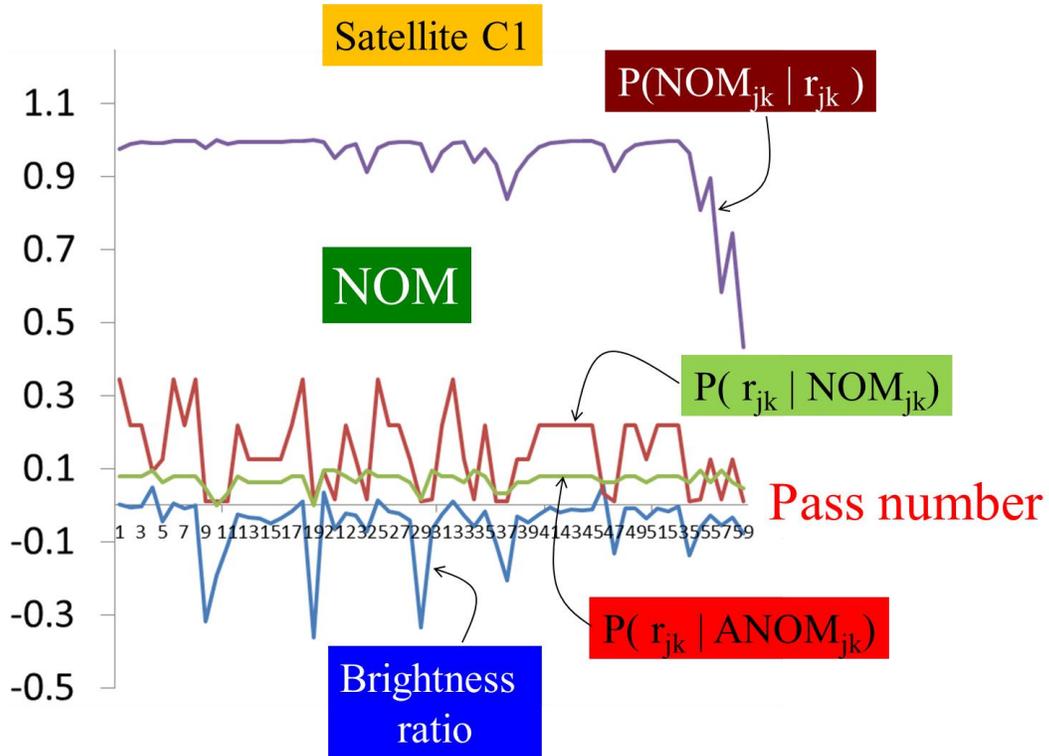
Figure B7a: Plot of $P(NOM_{jk} | r_{jk})$ for new data ($k \geq 0$) when satellite C1 is correctly tagged
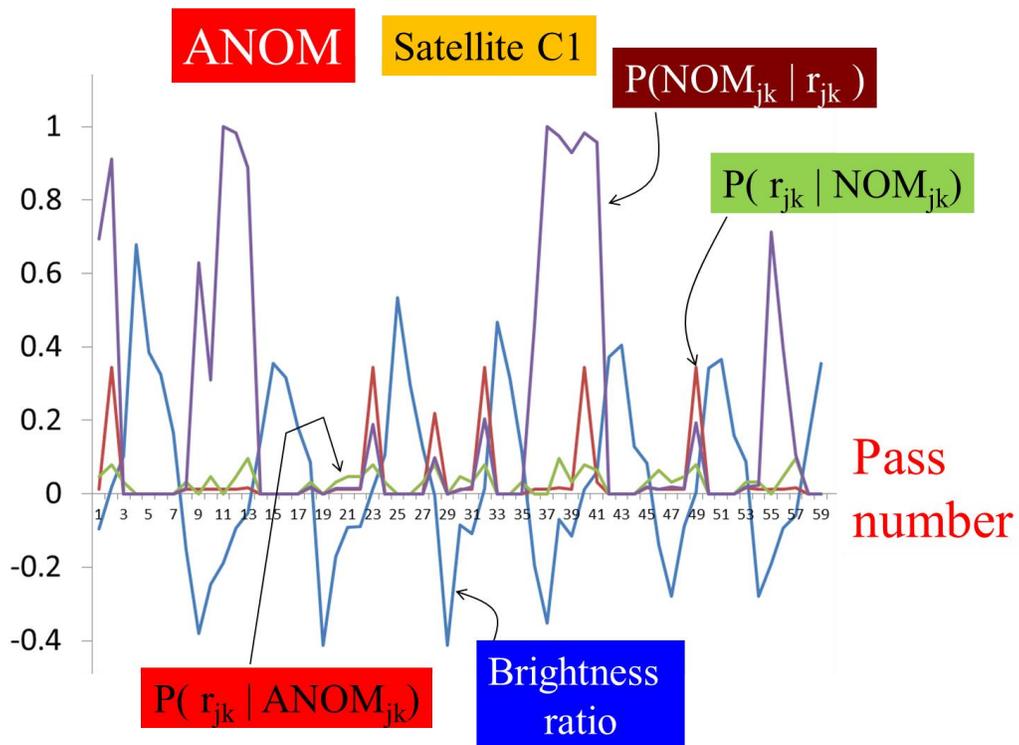
Figure B7b: Plot of $P(NOM_{jk} | r_{jk})$ for new data ($k \geq 0$) when satellite C1 is cross-tagged
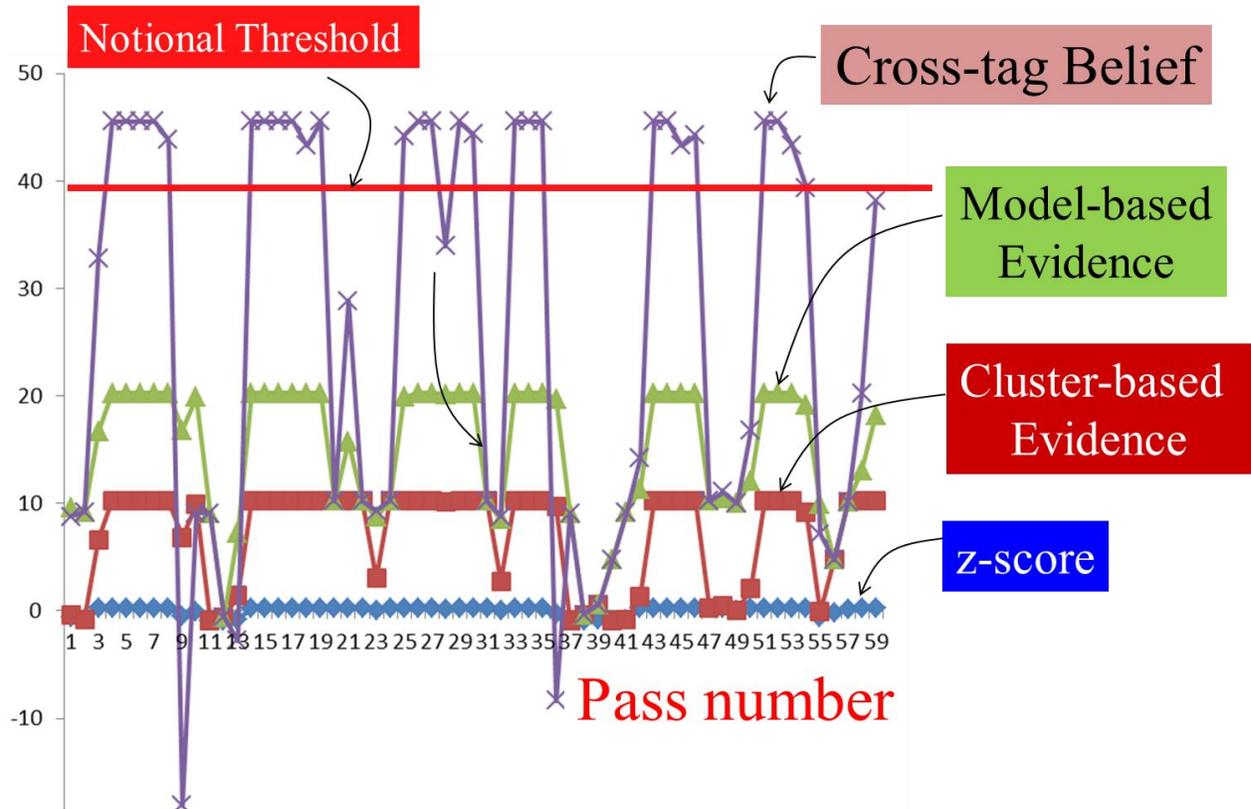
Figure B7c: Plot of belief that satellites C1 and C2 have been cross-tagged